# Physical Properties and Processes of Secondary Organic Aerosol and its Constituents

**Kent Salo**

**THESIS FOR THE DEGREE OF DOCTOR OF PHILOSOPHY IN NATURAL SCIENCE, SPECIALISING IN CHEMISTRY**

UNIVERSITY OF GOTHENBURG

**DEPARTMENT OF CHEMISTRY**
**UNIVERSITY OF GOTHENBURG**
**GÖTEBORG, SWEDEN, 2011**

Physical Properties and Processes of Secondary Organic Aerosol and its Constituents

Kent Salo



ISBN 978-91-628-8378-2
Available online at http://hdl.handle.net/2077/27778

Department of Chemistry
University of Gothenburg
SE-412 96 Göteborg
Sweden

Printed by Kompendiet AB
Göteborg, Sweden 2011

## Abstract

Atmospheric aerosol particles are involved in several important processes including the formation of clouds and precipitation. A considerable fraction of the ambient aerosol mass consists of organic compounds of both primary and secondary origin. These organic compounds are often semi-volatile and susceptible to oxidation which makes the organic aerosol a dynamic system, both chemically and physically. Once an aerosol is formed or released into the atmosphere, several processes will begin to alter its chemical and physical properties.

The focus of the work presented in this thesis has been to use experimental methods to characterise single aerosol components and more complex experimental systems, involving the formation and processing of secondary organic aerosol (SOA). The volatility of aerosol particles, e.g. the evaporation rate of the particles upon heating, can provide information of several important properties. From an aerosol consisting only of one pure compound it is possible to derive physical quantities like saturation vapour pressure and enthalpy of evaporation. In more complex systems like a secondary organic aerosol the volatility can give information about changes in composition, state of oxidation and degree of internal or external mixing.

With the use of a volatility tandem differential mobility analyser (VTDMA), the saturation vapour pressures and enthalpies of evaporation have been determined for pure compounds that are known constituents of ambient aerosol samples i.e. nine carboxylic acids. Two of them were cyclic, pinic and pinonic acid and seven of them were straight chain dicarboxylic acids with number of carbons ranging from $C_4$ to $C_{10}$. These properties were in addition evaluated for the aminium nitrates of mono-, di-, and trimethylamine, ethyl- and monoethanolamine. The calculated saturation vapour pressures for the carboxylic acids were in the range of $10^{-6}$ to $10^{-3}$ Pa and the determined enthalpies of evaporation ranged from 83 to 161 kJ $mol^{-1}$. The corresponding values for the aminium nitrates were for the calculated saturation vapour pressures approximately $10^{-4}$ Pa and for the enthalpies of evaporation 54 to 72 kJ $mol^{-1}$.

The VTDMA system has also been utilised to characterise SOA formed in the AIDA and SAPHIRE smog chambers from the ozonolysis of α-pinene and limonene and the change in the SOA thermal properties during OH radical induced ageing. Further, the effect of elevated ozone concentration and radical chemistry on SOA formed from limonene ozonolysis in the G-FROST laminar flow reactor was investigated. In addition, to compare with vapour pressures of aminium nitrates SOA generated from photooxodation of alkyl amines have been characterised in the EUPHORE smog chamber.

The calculated vapour pressures of all the investigated pure compounds in this work characterise them to be in the semi-volatile organic compound (SVOC) category; hence they will be present both in the gaseous and condensed phase in the atmosphere. This implied that all these compounds will be susceptible for gas phase OH radical oxidation that was demonstrated to be an important process for the complex mixtures investigated in the smog chamber facilities. The OH chemistry was also influencing the volatility of aerosol produced in G-FROST by ozonlysis. Regarding photooxodation of amines the aerosols produced under high $NO_x$ conditions initially mimicked the pure salts but was efficiently transformed by oxidation into an aerosol with similar volatility properties as observed in the terpene oxidation experiments.

Keywords: SOA, ageing, VOC, atmosphere, volatility, VTDMA, monoterpenes

## List of papers

Paper I

**Aerosol volatility and enthalpy of sublimation of carboxylic acids**

Salo, K., Å. M. Jonsson, P. U. Andersson and M. Hallquist (2010).
The Journal of Physical Chemistry A 114(13): 4586-4594

Paper II

**Thermal characterization of alkyl aminium nitrate nanoparticles**

Salo, K., J. Westerlund, P. U. Andersson, C. J. Nielsen, B. D'Anna and M. Hallquist (2011).
The Journal of Physical Chemistry A.115 (42): 11671-11677

Paper III

**Volatility of secondary organic aerosol during OH radical induced ageing**

Salo, K., M. Hallquist, Å. M. Jonsson, H. Saathoff, K. H. Naumann, C. Spindler, R. Tillmann, H. Fuchs, B. Bohn, F. Rubach, T. F. Mentel, L. Müller, M. Reinnig, T. Hoffmann and N. M. Donahue (2011).
Atmospheric Chemistry and Physics Discussions 11(7): 19507-19543

Paper IV

**Aging of secondary organic aerosol: connecting chambers to the atmosphere**

Donahue, N. M., K. M. Henry, T. F. Mentel, H. Saathoff, T. Hoffmann, K. Salo, T. Tritscher, P. B. Barmet, M. Hallquist, P. F. DeCarlo, J. Dommen, A. S. H. Prevot and U. Baltensperger (2011). Submitted to Proceedings of the National Academy of Sciences.

Paper V

**The influence of ozone and radical chemistry on the volatility of the secondary organic aerosol from limonene ozonolysis**

Salo K, R.K. Pathak, E.U. Emanuelsson, A. Lutz, Å. M. Jonsson and M. Hallquist (2011).
Manuscript for Environmental Science and Technology.

## Preface

Aerosol particles in the atmosphere have a large impact on our everyday life. These airborne microscopic particles have an effect on both health and climate and origin from a large variety of sources. In urban environments, e.g. in megacities, high concentrations of particles influence the health and the well being of the citizens. Aerosol particles from combustion processes and industrial activities are known to e.g. reduce visibility and cause premature deaths of thousands of people globally (Pope et al. 2006; Russell et al. 2009). The climate effect is partly direct by scattering light, causing so called global dimming and partly indirect, affecting cloud formation processes. The number of particles present will affect the size of the cloud droplets and hence cloud lifetime and amount of precipitation. In the fourth assessment report from the International Panel on Climate Change (IPCC 2007) (Solomon et al. 2007) the knowledge of these direct and indirect processes are described as scarce with a "low level of scientific understanding". In addition to anthropogenic sources of aerosol particles, biogenic sources also contribute to both particle number and mass. A significant fraction of this contribution is formed from chemical conversion of reactive volatile organic compounds (VOCs) emitted by plants. Many plants e.g. several of the species within the coniferous forests, covering a large part of the northern hemisphere, emit VOCs as a part of their metabolism. Reactive VOCs like terpenes are after emission oxidised and some of the products of these reactions will have lower vapour pressures and can form new particles and/or condense on present background particles. Characterisation of the ambient aerosol composition has shown that as much as 50% of the mass can be organic and that a considerable fraction of the organic matter is of secondary biogenic origin (Kanakidou et al. 2005). The metabolism and other processes controlling the release of VOCs from plants are often temperature dependent. This means that predicted future climate changes can result in complicated, possibly both positive and negative, biosphere-atmosphere-climate feedback mechanisms (Arneth et al. 2010; Peñuelas et al. 2010). The work in this thesis was done to increase the level of understanding of the processes behind the formation and fate of biogenic secondary organic aerosols (BSOA). This work concerns the physical and chemical properties of known organic aerosol constituents, with a focus on vapour pressures, partitioning between the gaseous and the condensed phase and the formation and ageing of nanosized aerosol particles. It was mainly done with laboratory studies using a volatility tandem differential mobility analyser (VTDMA) system. This system was applied at several of the most important smog chambers in Europe (AIDA, SAPHIRE, and EUPHORE) and at the G-FROST facility at the University of Gothenburg.

## Content

# 1. Introduction

**Question:** What is of the corresponding thickness of the peel of an ordinary apple and has the power to stop radiation, meteors and keep you warm in space?

**Answer:** The Atmosphere!

## 1.1 The Atmosphere

When viewing our planet Tellus from space it is easy to see that something distinguishes it from all other known planets. Our planet is beautiful blue and sparkles with life, a planet with the right conditions for life to exist and evolve. The most important differences between the Earth and our neighbour planets in the solar system are presence of water and the atmosphere. The atmosphere not only supplies us with oxygen it also protects us from UV-radiation from the sun and cosmic radiation, and by acting as the glass in a greenhouse it captures the outgoing long wave radiation keeping us warm in the cold space.

The outermost part of the atmosphere on the border to space is called the *thermosphere* reaching down to 80 km of height. In the outer part of the thermosphere the temperature can exceed hundreds of degrees Celsius due to the intense solar radiation and few molecules existing there, but the temperature drops with the altitude. The part of the atmosphere from 80 down to 50 km is called the *mesosphere*. The mesosphere is a very thin part of the atmosphere but despite this it is here most of the meteors burns up when entering the atmosphere from space. The next layer of the atmosphere is the *stratosphere*. Here the temperature increases with the altitude due to the absorption of shortwave radiation by ozone and oxygen. The absorption of UV-radiation ($\lambda < 240$ nm) cleaves oxygen molecules and forms oxygen atoms that gives ozone in reactions with molecular oxygen creating the protective ozone layer. The ozone molecules are photolysed by UV-radiation of longer wavelengths ($\lambda < 320$ nm). The "ozone cycle" is described by reaction 1.1 to 1.5 where (*) denotes existed state.

$$O_2 + h\nu\ (\lambda < 240\ \text{nm}) \rightarrow 2O^* \quad 1.1$$
$$O + O_2 + M \rightarrow O_3 + M \quad 1.2$$
$$O + O_3 \rightarrow 2O_2 \quad 1.3$$
$$O_3 + h\nu\ (\lambda < 320\ \text{nm}) \rightarrow O_2 + O^* \quad 1.4$$
$$O^* + M \rightarrow O + M \quad 1.5$$

It is in the lower part of the stratosphere, around 15-35 km where these essential reactions occur creating a steady state ozone concentration. The ozone reaction cycle involves release of excess energy via collision with a random molecule (M), thus creating a warming effect

(Finlayson Pitts et al. 2000). It is the increase in temperature with altitude induced by the photochemical formation of ozone that creates a stable, stratified layer of the atmosphere with very little vertical movements. When constituents from the air closer to the surface, like particles from volcano eruptions or persistent chemical compounds, enter the stratosphere they will be long-lived there due to the lack of vertical movements and precipitation. A long lifetime and efficient horizontal movements will distribute a compound in the stratosphere globally.

*The troposphere* is the atmospheric layer that extends from the surface up to the stratosphere, 9 to 17 km's height depending on latitude, season and weather. The troposphere is well mixed due to convection and winds. In fact the name troposphere origins from the Greek word for overturn: trope (τροπή). The convection originates from the fact that energetic shortwave radiation from the sun heats the Earth's surface that will subsequently emit longwave radiation and thus heat the moist air closest to the ground. This heating causes air masses to rise and thereby transport for example water vapour and aerosol particles higher up in the troposphere. As a rising "air-parcel" expands due to the reduced pressure it cools down and the air might get supersaturated with respect to water that then will condense on aerosol particles and create clouds. When water condense to form clouds latent heat is released causing even more convection. The result is that the troposphere is characterised by complex weather systems that propagate globally. The troposphere contains 90% of the mass of the atmosphere. Here the main components of dry air are 78.08% nitrogen, 20.90% oxygen and 0.93% argon. The water content varies from almost zero to 4% depending on altitude, latitude and temperature (Lutgens et al. 2004). The troposphere contains in addition a number of trace gases typically in the concentration range of parts per billion (ppb) and parts per million (ppm), where the most important examples are hydrogen, carbon dioxide ($CO_2$), nitrous oxides ($NO_x$), sulphur dioxide ($SO_2$), ammonia ($NH_3$), methane ($CH_4$), and volatile organic compounds (VOC). These gaseous compounds can originate from both natural and anthropogenic processes and their tropospheric lifetimes are dependent on their reactivity. The troposphere has a strong oxidative potential and all reactive compounds emitted here will in course of time get oxidised, become more polar and be removed by wet or dry deposition. The most important atmospheric oxidants are ozone ($O_3$), OH radicals (day-time), $NO_3$ radicals (night-time) and Cl atoms (marine environment). There is episodically down mixing of stratospheric ozone but the main source of tropospheric ozone is the photolysis of $NO_2$ produced mainly from human activities. When $NO_2$ is photolysed, atomic oxygen is formed (1.6), which will react with molecular oxygen to form ozone (1.7).

$$NO_2 + h\nu\ (\lambda < 430\ nm) \rightarrow NO + O \qquad 1.6$$
$$O_2 + O + M \rightarrow O_3 + M \qquad 1.7\ (1.2)$$
$$O_3 + NO \rightarrow O_2 + NO_2 \qquad 1.8$$
$$O_3 + h\nu\ (\lambda < 340\ nm) \rightarrow O_2 + O^* \qquad 1.9\ (1.4)$$

Major sinks of ozone are reaction with NO and photolysis, reactions 1.8 and 1.9. In the latter exited O is formed that, if not quenched back to ground state by collision (1.5), can react with water forming OH radicals (1.10) (Seinfeld et al. 2006).

$$O^* + H_2O \rightarrow 2\ OH \qquad 1.10$$

The $NO_3$ radical is readily photolysed in daylight but it is an important oxidant during night time. It is formed from the $NO_2$ reaction with $O_3$ (1.11).

$$NO_2 + O_3 \rightarrow NO_3 + O_2 \quad 1.11$$

Because of reaction 1.8 high concentrations of ozone and NO cannot co-exist, and the net outcome of the series of reactions described in 1.6 to 1.11 will be a rather low steady state concentration of ozone in the troposphere (Finlayson-Pitts et al. 2000). The oxidants described above in combination with several radical processes are involved in the oxidation of VOCs in the troposphere where NO is converted to $NO_2$ without consumption of ozone (1.12–1.16). This leads to excessive ozone levels but also to oxidised organic products with potential harmful properties. The VOC is denoted (RH) and forms an alkyl radical (R) in reaction 1.12.

$$RH + OH \rightarrow R + H_2O \quad 1.12$$
$$R + O_2 \rightarrow RO_2 \quad 1.13$$
$$RO_2 + NO \rightarrow RO + NO_2 \quad 1.14$$
$$RO + O_2 \rightarrow \text{carbonyl} + HO_2 \quad 1.15$$
$$HO_2 + NO \rightarrow OH + NO_2 \quad 1.16$$

In polluted areas the formation of "photochemical smog" has been and still is a big problem and was early connected to the emissions of VOCs and nitrogen oxides ($NO_x$) mainly from urban traffic sources (Fenger 2009). Some of the products from these reactions will be ozone, oxygenated VOCs like carboxcylic acids and aldehydes, organic nitrate compounds like peroxy acetyl nitrate (PAN), inorganic acids and particles. This smog will be seen as a brownish haze that reduces the visibility in many urban areas. A summary of main reactants and typical products in photochemical smog are shown in reaction 1.17.

$$VOC + NO_x + h\nu \rightarrow O_3 + HNO_3 + PAN + HCHO + HCOOH + \text{particles, etc.} \quad 1.17$$

A more detailed description of the OH initiated oxidation of VOC is done separately (see section 1.2.2 Atmospheric VOC chemistry)

## 1.2 Volatile Organic Compounds (VOC)

### 1.2.1 Emissions and impact

There exists numerous different organic compounds and their complex chemistry is the very base of the chemistry of life. The main constituents are carbon, hydrogen and oxygen but also nitrogen, sulphur and halogens are important building blocks. The number of possible conformations (isomers) increases dramatically with the number of carbon atoms. An organic compound containing only 10 carbon atoms ($C_{10}$) have 100 possible isomers and if other compounds or functional groups are added the complexity increases enormously (Goldstein et al. 2007). Gaseous organic compounds that can be found in the atmosphere are commonly referred to as volatile organic compounds (VOC). A large fraction of VOC in the atmosphere is from human activities, i.e. of anthropogenic origin, and examples of sources are

fossil fuels, petrochemical processes, biomass burning, food production and animal husbandry. The characteristics of anthropogenic VOC sources are changing with time and implementation of new technology may include new types of VOC emissions. For example, there has recently been a large interest in techniques used to capture and store $CO_2$ to reduce the emission of this important greenhouse gas. One of the $CO_2$ capture techniques is amine-based, i.e. aquatic solutions of amines are used to chemically bond $CO_2$ in the exhausts from power plants fired with fossil fuel. If implemented worldwide this could possibly lead to a significant new source of amines to the atmosphere (Thitakamol et al. 2007). Regarding biogenic VOC emissions, they are on a global level significantly larger in mass and are emitted by vegetation during their growth as by-products from their metabolisms and during the decay of the plant (Goldstein et al. 2007). A schematic mass balance of the global VOC budget expressed in teragram carbon per year (Tg C $yr^{-1}$) is seen in Figure 1 (Goldstein et al. 2007; Hallquist et al. 2009). The total emissions of VOC to the atmosphere are estimated to be 1350 Tg C $yr^{-1}$ where the biogenic contribution is 1150 Tg C $yr^{-1}$ (Guenther et al. 1995). It is estimated that 800 Tg C $yr^{-1}$ are lost by gas phase wet and dry deposition, 300-500 Tg C $yr^{-1}$ are oxidised to CO and $CO_2$ and 150 Tg C $yr^{-1}$ are transferred into particulate mass, i.e. secondary organic aerosol (SOA) production. The SOA particles formed in these processes are mainly lost due to wet and dry deposition (Hallquist et al. 2009). It is also possible for compounds that contribute to the SOA mass to evaporate back to VOCs, due to changes in partitioning or condensed phase chemical transformation.

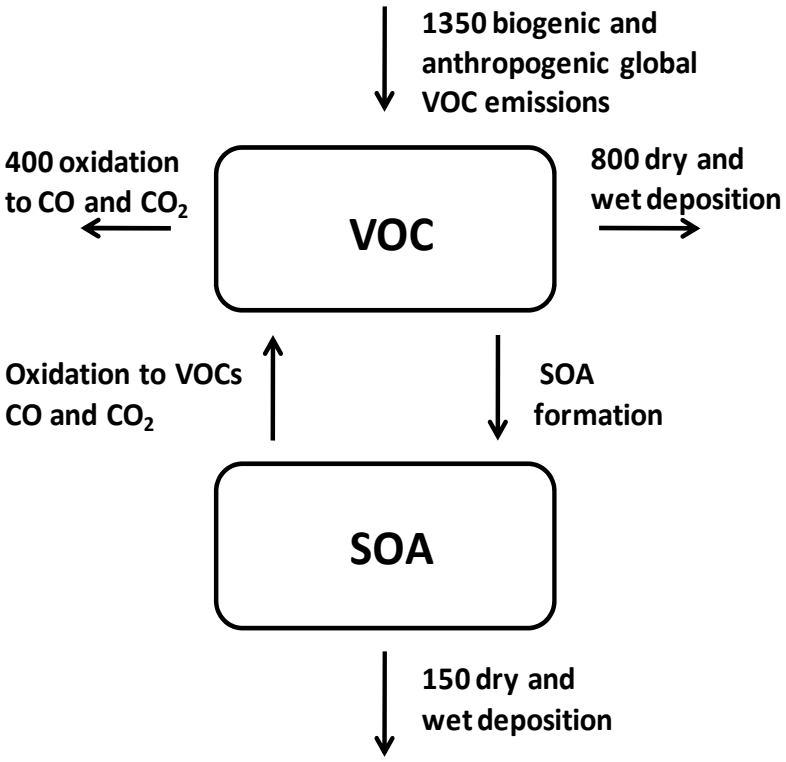


**Figure 1** Globally estimated VOC mass balance in Tg C $yr^{-1}$ (Goldstein et al. 2007; Hallquist et al. 2009)

It is very hard to generalise the effect of VOCs in the environment due to their diverse structure and properties. However, regarding potential negative health effects many compounds are direct toxic and carcinogenic. Since the anthropogenic emissions of VOCs mainly occur within populated areas they generally posing a larger treat for enhanced human exposure than those emitted from biogenic sources. Additionally, VOCs play an important role when it comes to climate, having the ability to act as powerful greenhouse gases but even more important is the indirect effect by being responsible for enhanced levels of tropospheric ozone, one of the most significant greenhouse gases. Another indirect climate effect of VOCs is their role as precursors to atmospheric aerosol formation, forming secondary organic aerosols (SOA). The topic of SOA is the core of this thesis and listed in Table 1 are examples of sources and estimated emissions in teragram ($10^{12}$) carbon yearly (Tg C $yr^{-1}$) or gigagram ($10^{9}$) nitrogen yearly (Gg N $yr^{-1}$) of the VOCs related to this work, either as a SOA precursor or as a typical SOA constituent.

**Table 1.** Sources and emissions for some of the VOCs investigated in this work.

| Compound | Emissions | Sources |
|---|---|---|
| **limonene** | 6-13¤, 1 | vegetation |
| **α-pinene** | 15-64¤, 1 | vegetation |
| **methylamine** | 83±26*, 2 | animal husbandry |
| **dimethylamine** | 33 ± 19*, 2 | animal husbandry<br>fish processing |
| **trimethylamine** | 169 ± 33*, 2 | animal husbandry |
| **monoethanolamine** | - | industry, $CO_2$-capture |
| **ethylamine** | - | animal husbandry<br>fish processing |

¤Tg C $yr^{-1}$, *Gg N $yr^{-1}$, [1](Geron et al. 2000; Schurgers et al. 2009), [2](Ge et al. 2011)

### 1.2.2 Atmospheric VOC chemistry

The lifetimes of VOC in the atmosphere are diverse and depend on the reactivity of each compound. It ranges from minutes for reactive unsaturated biogenic compounds to several years for anthropogenic persistent molecules like chlorofluorocarbons i.e. freons. Besides wet and dry deposition VOCs are removed from the atmosphere by photolysis and chemical reactions. The predominant route during daytime is the reaction with OH radicals. Figure 2 illustrates a schematic of the OH radical initiated VOC oxidation. This is an extension of the previous described VOC reaction scheme (1.12-1.16).

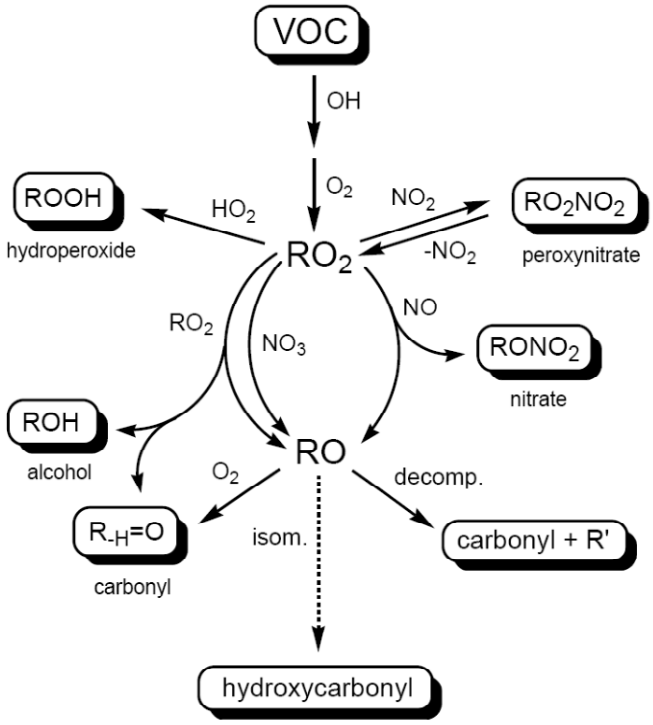


**Figure 2** Sequence of OH radical initiated VOC oxidation, adapted from Hallquist et al. (2009).

For a saturated VOC the OH radical reaction starts by the removal of a hydrogen atom from the VOC molecule leading to the formation of an alkyl radical (R) and water. This is followed by the fast addition of $O_2$ to the alkyl radical to form a peroxy radical ($RO_2$). Under high $NO_x$ conditions the $RO_2$ radical is readily converted to an alkoxy radical (RO) via the oxidation of NO to $NO_2$. Larger $RO_2$ radicals can form stable organic nitrates from the reaction with NO. Under low $NO_x$ conditions the $RO_2$ radical reaction with $HO_2$ to form a hydroperoxide or with another $RO_2$ radical to form RO or products such as alcohol and carbonyls becomes important. The $RO_2$ radical can also be temporally trapped and subject for long range transport by its reaction with $NO_2$ to form peroxy nitrate e.g. peroxyacetyl nitrate (PAN). The RO radical reacts, isomerises or decomposes to carbonyl or hydroxyl carbonyl products. Several of the species formed in these reactions will take part in further reactions to form a wide array of products in the atmosphere. Which products that will be the outcome of the OH radical initiated VOC degradation will for example depend on the $NO_x$ level, temperature, relative humidity (RH) and on the precursor VOC. The rate of the reaction between OH radicals and larger alkanes is within an order of magnitude of the diffusion limit (Atkinson et al. 2008). The OH radicals react with alkenes through addition to the double bond, forming an alkyl radical that will form a $RO_2$ radical with $O_2$ in a similar way as the alkyl radical formed from alkanes (Figure 2). These $RO_2$ radicals will undergo the same reaction as described earlier. The OH radical reaction with amines occurs in a similar way but with the additional possibility of the abstraction of the N-hydrogen, yielding an alkylamino radical that will promptly react further to form a wide range of nitrogen containing organic products, e.g. amides, nitrosamides and nitramines. Besides the reaction with OH radicals, alkaline VOCs like amines will also be removed from the atmosphere through reaction

with acids or being subject to uptake on acidic aerosols hence contributing to the aerosol mass via salt formation.

Another important atmospheric oxidant for unsaturated compounds is ozone. The ozone reaction with alkenes occurs with a several orders of magnitude lower reaction rate than the reaction with OH but it is anyway an important sink for alkenes in the atmosphere due to the higher concentrations of ozone compared to OH radicals ($O_3$ ~$10^{11}$-$10^{12}$ molecules $cm^{-3}$, OH radicals ~ $10^5$-$10^6$ molecules $cm^{-3}$) especially in the remote, unpolluted atmosphere (Finlayson-Pitts et al. 2000). The ozone reaction with alkenes starts with the addition of ozone to the carbon-carbon double bond leading to formation of a primary ozonide. The primary ozonide is not stable in the gas-phase and will quickly decompose, producing a carbonyl molecule and a carbonyloxide known as a Criegee Intermediate (CI). The CI will react further to produce the first generation of stable products. The reaction of the CI has a substantial OH yield and will play an important role in the further oxidation of the initially formed products and the precursor (Johnson et al. 2008). The structure of the CI formed and thereby the product distribution is highly dependent on the structure of the precursor molecule. In the same way as for the OH radical reaction with VOCs the products formed from the ozone reaction with alkenes is highly dependent on the $NO_x$ concentration but also on water (RH) and reaction temperature (Johnson et al. 2008; Jonsson 2008; Jonsson et al. 2006; Jonsson et al. 2008a, 2008b).

The atmospheric oxidation of a VOC will produce products with other physical and chemical properties, e.g. the polarity, molecular weight and saturation vapour pressure ($p^0$), compared to the parent compound. The saturation vapour pressure is the partial pressure at a given temperature of a pure compound when it is in equilibrium considering evaporation/condensation. Generally, the oxidation products can be divided with regards to their volatility, i.e. related to their potential contribution to particle mass by partitioning: VOCs (>1 Pa), found only in the gas phase; intermediate-volatile organic compounds (IVOC, 1-$10^{-2}$ Pa), found predominately in the gas phase; semi-volatile organic compounds (SVOC, $10^{-2}$-$10^{-8}$ Pa) present both in the gas and the condensed phase and low-volatile organic compounds (LVOC, <$10^{-8}$ Pa), found in the condensed phase.

## 1.3 Particles

### 1.3.1 Definition, sources and composition

After the eruption of Eyjafjallajökull in 2010 that left thousands of flights on the ground; the effect of aerosol particles on our daily life was apparent. Less apparent but very important in our daily life is the aerosol particle effect on human health and their interactions with Earth's climate (Pöschl 2005). The definition of an aerosol is liquid or solid particles suspended in a surrounding gas, usually air (Hinds 1999). Tropospheric particle number concentrations vary from $10^2$ $cm^{-3}$ in remote areas to $10^8$ $cm^{-3}$ in polluted urban areas. The size of the aerosol particles suspended in the atmosphere can range from a few nanometres up to hundreds of micrometers. Aerosol particles are often defined by size and divided into different size-ranges. In Figure 3 a schematic presentation of the atmospheric aerosol size distribution, sources and sinks are displayed. The smallest particles from 3 to 80 nm are called the Aitken mode and the sources of these particles are condensation of hot vapours e.g. at the end of an exhaust pipe or atmospheric nucleation involving water, sulphuric acid and oxidised organic molecules (Kulmala et al. 2004). The Aitken

mode particles are lost by diffusion and by coagulation to larger particles. The lifetime of these smallest particles are relatively short and ranges from minutes to hours. The size range from 80 to 1000 nm is called the accumulation mode and is formed from the coagulation but also from condensational growth of the smaller Aitken mode particles. The accumulation mode particles have low rate of coagulation and sedimentation and thereby the longest atmospheric lifetime, more than several days and the primary sink is rainout and washout. The largest particles, the coarse mode, are mostly mechanically generated and with enough mass to be removed from the atmosphere by sedimentation within few hours, but can during some conditions be transported long distances over several days. The Aitken mode particles contribute the most to aerosol number concentrations while the coarse particles contribute the most to mass.

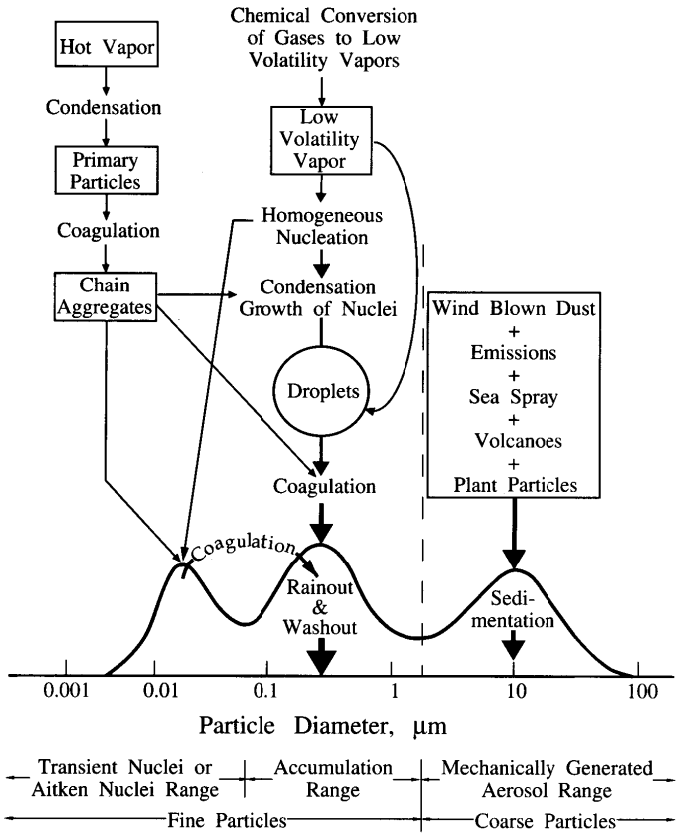


**Figure 3** A Schematic of the distribution of an atmospheric aerosol and its sources and sinks, adapted from "Atmospheric Chemistry and Physics" (Seinfeld et al. 2006).

### 1.3.2 Secondary Organic Aerosol (SOA)

There is a difference between primary particles that are released directly into the atmosphere and secondary particles that are formed by atmospheric processes. New particles are formed from nucleation of low vapour pressure compounds i.e. sulphates, nitrates or oxidised organic compounds. These compounds originate from gases that are converted to form products of low volatility by chemical reactions. The gaseous compounds most subjected to this are $SO_2$, $NO_x$

and reactive VOCs. The VOCs that are gaseous under atmospheric conditions will become less volatile by the increased molecular masses and polarity induced by oxidation reactions. If these oxidation products are LVOC and reach high enough concentrations they can participate in new particle formation forming new SOA particles and contribute to the particle number concentration. New particle formation events (nucleation events) have been observed globally in many locations e.g. remote forests, industrial regions and megacities (Kulmala et al. 2004). SOA can also contribute to aerosol mass, the SVOC and LVOC formed in atmospheric oxidation reactions can condense on or partitioning into existing particles. As described in connection to Figure 1, this formation of secondary organic aerosol contribute to an important fraction of the aerosol mass on a global scale. The condensation and evaporation are reversible processes and are controlled by the saturation vapour pressures of the aerosol constituents and concentration of the aerosol in a non-reactive system. Secondary aerosols can also be formed by gaseous acid-base reactions of ammonia, amines or other bases with inorganic acids like $HNO_3$, $H_2SO_4$ and HCl or organic acids. The products from these acid-base reactions will be watersoluble semi- or low-volatile salts.

Regarding the SOA of interest to the work presented in this thesis, it has been shown that the uptake of ammonia and organic amines to acidic aerosols will contribute significant to the total SOA mass (Smith et al. 2010) and possibly also to atmospheric nucleation (Kurtén et al. 2008). The oxidation of biogenic precursors, e.g. the monoterpenes investigated in the current study, is a large source of atmospheric dicarboxylic acids (Claeys et al. 2007; Ma et al. 2007; Müller et al. 2011). As a result of their own measurements and a comprehensive literature study, Zhang et al. (2010) reported that dicarboxylic acids account for as much as 11% of the water soluble organic compounds (WSOC) in an atmospheric aerosol.

### 1.3.3 Health

There are severe health effects connected to increased particle mass and number concentration in the atmosphere. The effect aerosol particles have on human health is firstly dependent on particle size due to penetration and deposition efficiency. The upper part of the human respiratory system efficiently removes coarse particles, predominantly in the bronchial regions causing symptoms connected to breathing. Smaller particles tend to reach deeper into the lungs. Recently several reports have stated that nanosized particles can pass through the defensive barriers of the respiratory system, entering the bloodstream and inducing stress to the immune system, leading to increased risks of cardiovascular diseases (Pope et al. 2006; Russell et al. 2009). It may be noted that humidification in the lung system can induce size changes and thereby the hygroscopicity and indirectly the chemical composition of the particles are also connected to the deposition efficiency in the lungs (Löndahl et al. 2009). Secondly, the particle constituents themselves can pose a threat e.g. the particles can act as carriers of toxic or mutagenic compounds like polycyclic aromatic hydrocarbons (PAH). There are also suggestions that the solubility of the particle material will be of importance concerning these issues e.g. that insoluble parts in aerosol particles possibly could led to increased risks of exposure (Imrich et al. 2000). Fibrous particles like asbestos are also well known to be carcinogenic and have caused countless premature deaths among industrial workers (Gravatt et al. 1977).

### 1.3.4 Climate

Aerosols have significant direct and indirect climate effects. The direct effects are scattering and reflection of radiation. Examples are reduced visibility and "global dimming" influencing the radiation budget of the Earth with a net cooling effect. Some particles can also provide a net heating effect by absorption of radiation, i.e. the case for soot or black carbon aerosols. In addition, the deposition of soot particles on ice and snow covered surfaces can lower the albedo and thereby contribute to additional warming. In the troposphere the climate direct effects of particles are very heterogeneously distributed due to the short days to week lifetime of particles. However, in the stratosphere the effect will be more globally distributed. For example volcano ash particles emitted to the stratosphere can be transported long distances and cause failure of crops globally due to their cooling effect. There are even serious suggestions to use the long stratospheric lifetime of particles too, by dispersion of ammonium sulphate aerosol in the lower stratosphere, counteract the global warming (Rasch et al. 2008).

The indirect effect is the aerosols influence on the presence and size distribution of cloud droplets, e.g. if more aerosol particles are available a larger number of smaller cloud droplets will be formed. Clouds that are composed of smaller droplets have other optical properties and will also have longer lifetimes. The indirect effects can cause possible altering of precipitation systems, possessing large and often unknown feedback mechanisms to the climate change (Solomon et al. 2007).

Since many of the SOA precursors are emitted from different biological processes i.e. BVOC, a global increase in for examples temperature will have an effect on the emission of SOA precursors, hence have a large effect on the amount of SOA produced. Since the composition of the precursors will control the composition of the biogenic SOA formed not only the mass but also the chemical and physical properties will be altered in a changing climate (Arneth et al. 2010; Peñuelas et al. 2010).

### 1.3.5 Atmospheric aerosol ageing and volatility

Once the aerosol particles are released to or formed in the atmosphere they will start to transform/age. Figure 4 shows the possible pathways of these ageing processes.

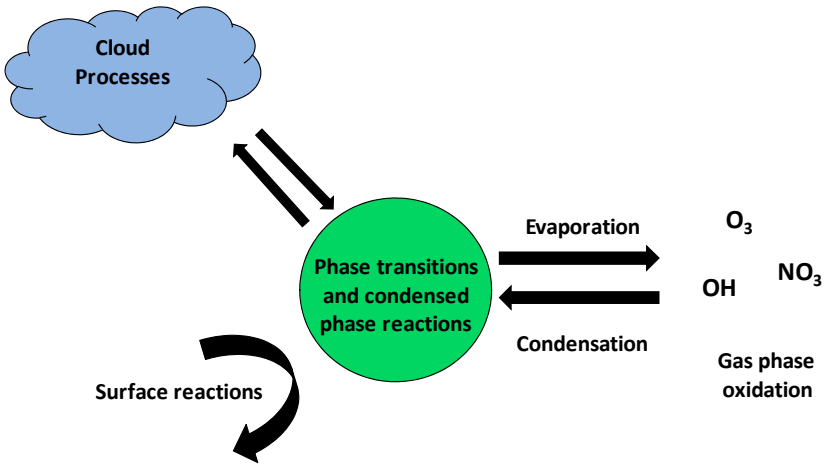


**Figure 4** The ageing processes of SOA particles.

*Cloud processes:* If the RH increases the aerosol particles will take up water and eventually droplets will form. Water soluble compounds in the droplets can then dissolve and aqueous chemistry will take place (Bateman et al. 2011). If these cloud droplets dry out cloud processed, internally mixed aerosol particles will be formed. Cloud processing will have a large influence on both chemical and optical properties of the aerosol, including hygroscopicity, refractivity and volatility (Pöschl 2011).

*Evaporation/Condensation*: *i.e. partitioning:* SVOCs in the particles and in the gaseous phase are subject to partitioning (evaporating and condensing). This partitioning depends on e.g. temperature, compound specific properties and available condensed organic matter. Evaporated SVOCs and other reactive compounds can undergo gas phase oxidation reactions, hence react with $O_3$, OH radicals, $NO_3$ radicals (night-time) or Cl atoms (marine environment). If these oxidation reactions do not lead to fragmentation of the molecules their vapour pressures will decrease and lead to the re-condensation/partitioning of these new compounds back into the condensed phase. This process will form an aged and internally mixed aerosol.

*Surface reactions:* Oxidation reactions can also occur at the surface of the particle e.g. the uptake of OH radicals (Lambe et al. 2009; Pöschl et al. 2007). Other types of surface reactions are the increase in aerosol mass by reactive uptake of ammonia or amines which will neutralise acidic aerosols or the exchange of ammonia for another base in ammonium salt aerosols as suggested by Loyd et al. (2009) and Smith et al. (2010).

*Condensed phase reactions:* There is also evidence of a number of chemical and physical processes within the particle e.g. change of physical state or the formation of macromolecules or polymers e.g. via acetal or amid formation (Barsanti et al. 2006; Chen et al. 2011; Hallquist et al. 2009; Kalberer et al. 2004). Especially at higher RHs there is evidence of formation of macromolecules (oligomers or polymers) (Barsanti et al. 2004, 2005, 2006; Tolocka et al. 2004). Liquid aerosol particles can also go through phase transitions and form highly viscous or glassy states. The physical state of an organic aerosol particle will have a large effect on the possibilities for and rates of any condensed phase reaction (Mikhailov et al. 2009; Pöschl 2011; Shiraiwa et al. 2011; Virtanen et al. 2010; Zobrist et al. 2008). There are also suggestions that the physical state of the aerosol will have an effect on the evaporation rate (Saleh et al. 2011; Saleh et al. 2009; Vaden et al. 2011).

The ageing processes described above will be reflected in the volatility of the SOA particles. The quantification of the volatility becomes a very useful tool to get insight into SOA chemistry, phase changes and other ageing processes. Today volatility is an established dimension to characterise ageing. Recently, a second dimension to describe ageing was introduced (Aiken et al. 2008). This is to parameterise the state of ageing of SOA by the ratio between the number of oxygen and carbon atoms in the particle (O/C). The higher O/C, the more oxidised are the SOA constituents and the more aged are the aerosol particles. The O/C is often derived using a high resolution aerosol mass spectrometer (AMS) (Jayne et al. 2000). This instrument can give on-line information of the ageing state of an organic aerosol with high time resolution. Figure 5 describes alternative oxidation paths when a reactive precursor gas e.g. α-pinene is oxidised; the oxidation leads to an increase in O/C. This oxidation can lead to fragmentation to smaller, more volatile molecules e.g. aldehydes or ketones, with $CO_2$ (O/C=2) as the ultimate end-product. In addition the oxidation can introduce functional groups i.e. functionalisation,

which increase the molecular weight and polarity making the molecule less volatile. This is illustrated in the figure where α-pinene is oxidised to pinic acid that gets further oxidised to the tricarboxylic acid 3-methyl-1,2,3,butanetricarboxylic acid, (MBTCA). All these oxidation steps increases the O/C. The volatility can also decrease via the formation of macromolecules e.g. oligomerisation without any effect on the O/C. Thus there is a need for both dimensions in order to describe the ageing processes.

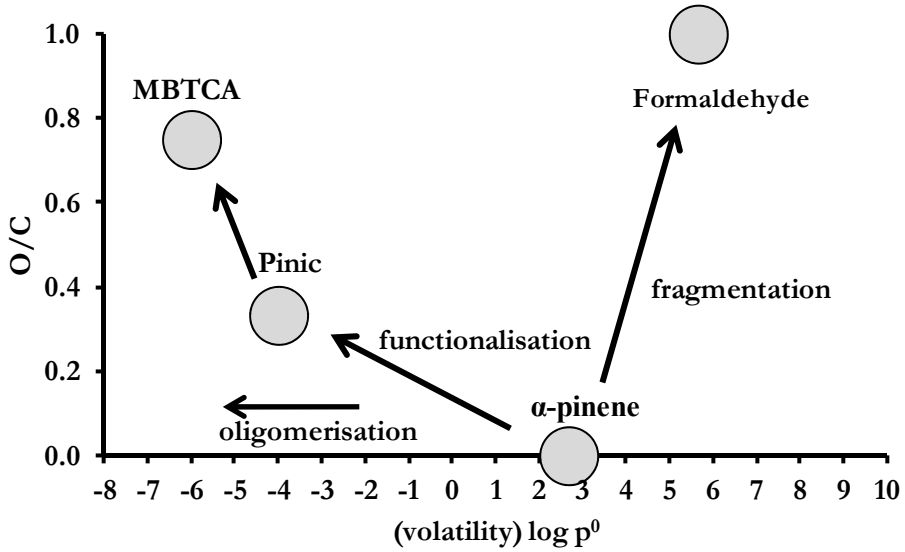


**Figure 5** Different paths of the oxidation of a VOC; functionalisation, leading to larger, less volatile molecules with increased O/C, fragmentation, leading to smaller, more volatile molecules with increased O/C and oligomerisation, forming larger, less volatile molecules, not necessarily affecting the O/C. (Figure inspired by Jimenez et al. (2009)

# 2. Theory

## 2.1 Partitioning

The distribution of a SVOC between the gaseous and condensed phase in the atmosphere is often described with the partitioning coefficient $K_p$ (Pankow 1994).

$$K_{p,i} = \frac{F_{i,om}}{A_i TSP} = \frac{RTf_{om}}{MW_{om}\zeta_i p_i^0} \quad 2.1.$$

In Equation 2.1, $F_{i,om}$ and $A_i$ are the condensed and gaseous concentrations of compound *i* and *TSP* is the concentration of the total suspended particulate matter. *R* is the common gas constant, *T* the temperature, $f_{om}$ is the weight fraction of the TSP that is the absorbing organic material, $MW_{om}$ the mean molecular weight of the absorbing organic material, $\zeta_i$ is the activity coefficient and $p^0_i$ is the saturation vapour pressure. Equation 2.1 shows that an SVOC will distribute between the condensed and gaseous phase not only depending on temperature and molecular properties but also on the total aerosol concentration. This means that the dilution of an SOA, reducing TSP will change the particle chemical composition by pushing compound *i* into the gas phase.

Another approach to describe the volatility distribution of the compounds in an aerosol is the Volatility Basis Set (VBS) as described by Donahue et al. (2006). The basis for this method is to lump the vast number of SOA constituents into "volatility bins". These bins are based on saturation vapour pressures of the different compounds, often expressed as $C_i^*$ (μg $m^{-3}$) and separated by factors of 10. The bins often range from 0.01 to 100 000 μg $m^{-3}$ covering the least volatile compounds in the atmosphere (entirely in the condensed phase under atmospheric conditions) to the most volatile (entirely present in the gaseus phase). The unit is dependent on the molecular weight, but it is assumed that the constituents have a mean molecular weight of ~ 200 g $mol^{-1}$(Donahue et al. 2006). In this way it is possible to treat the complex mixture of hundreds of compounds with few volatility bins. Figure 6 shows the volatility distribution of the products from an α-pinene ozonolysis experiment. The white bars show gas phase compounds and the green bars the products in the condensed phase in the presence of 66.3 μg $m^{-3}$ organic aerosol.

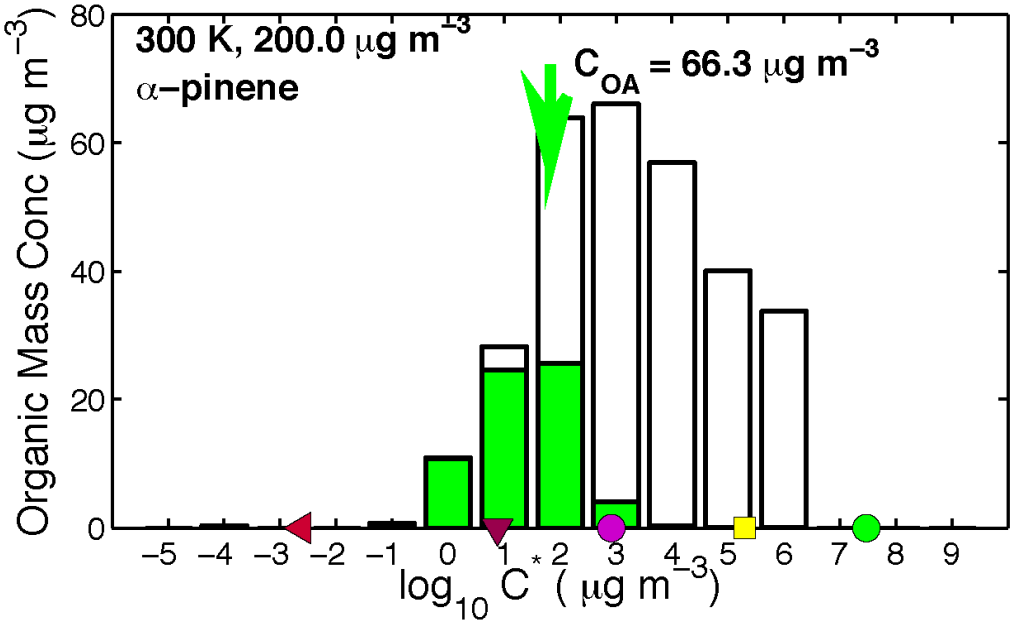


**Figure 6** Example of a collection of semi-volatile compounds,(first generation α-pinene ozonolysis products) with total mass concentrations shown with full bars and the condensed-phase portion with filled (green) bars according to their logarithmic saturation vapour pressures (log C*). The coloured symbols show the logarithmic saturation vapour pressures (log C*) for α-pinene (green circle) and the oxidation products measured during MUCHACHAS, pinonaldehyde (yellow square), pinonic acid (magenta circle), pinic acid (maroon downward triangle) and MBTCA (red leftward triangle) adapted from Paper IV .

## 2.2 Evaporation

The phase transition from a liquid aerosol particle to the gas phase is defined as vaporisation and from a solid particle as sublimation. The energy needed to transfer one mole of a compound between the condensed phase and the gaseous phase is called enthalpy of vaporisation/sublimation. The volatility of a SOA particle is dependent on its phase, composition and the interactions between its constituents. In the work herein the word evaporation is used in parallel with sublimation or vaporisation to describe the gas transition from amorphous or unknown phases.

The non-equilibrium evaporation from an aerosol particle consisting of a single compound can with the assumptions that 1) the particle is spherical with isotropic surface free energy and 2) the vapour pressures from the evaporated species and any latent heat are negligible, be described as:

$$\frac{dD_p}{dt} = -\frac{4D_{i,air}M_i}{\rho_i D_p RT}\, p_i^0 \exp\left(\frac{4\gamma_i M_i}{D_p \rho_i RT}\right) f(Kn_i, \alpha) \qquad 2.2$$

In Equation 2.2 $D_p$ is the particle diameter, $D_{i,air}$ is the diffusivity of compound $i$ in air. $M_i$ is the molar mass of $i$ and $\rho_i$ is the density. $R$ the gas constant, $T$ the temperature, $t$ the evaporation

time and $\gamma_i$ is the surface free energy. $f(Kn_p, \alpha)$ is the semi empirical Fuchs and Sutugin correction term for particle diameters in the non continuous e. g. transition regime (Fuchs et al. 1971).

$$f\left(Kn_i,\alpha\right)=\frac{1+Kn_i}{1+0.3773\times Kn_i+1.33\times Kn_i\times\frac{\left(1+Kn_i\right)}{\alpha}} \quad 2.3$$

In Equation 2.3 $\alpha$ is the mass accommodation or evaporation factor. In the case of evaporation this factor describes the inertia in the evaporation process e.g. evaporation coefficient. Recent publications discuss the magnitude of this quantity in evaporation processes (Riipinen et al. 2010; Vaden et al. 2011). However in this work it was set to unity meaning that all "evaporation events" are successful. $Kn_i$ is the Knudsen number a dimensionless number defined in Equation 2.4. It is the ratio between the mean free path ($\lambda$) and the particle diameter ($D_p$). A $Kn_i \rightarrow 0$ indicates continuum regime, $Kn_i \rightarrow \infty$ free molecule (kinetic) regime and $Kn_i \sim 1$ indicates that the mass flux occurs in the transition regime. The mean free path $\lambda_{air}$(298K) is 66 nm meaning that 10 nm < $D_p$ < 200 nm belongs to the transition regime (Seinfeld et al. 2006).

$$Kn=\frac{2\lambda_i}{D_p} \quad 2.4$$

The diffusivity of species *i*, in air $D_{i,air}$, is given by Equation 2.5

$$D_{i,air}=5.9542\times10^{24}\frac{\sqrt{T^3\left(\frac{1}{M_i}+\frac{1}{M_{air}}\right)}}{p\sigma_{i,air}^2\Omega_{i,air}} \quad 2.5$$

where $M_i$ is the molar mass, $p$ is the total pressure and $\sigma_i$ is the inter-particle distance where the potential is zero derived from the critical volume ($V_{c,i}$) of *i* as $\sigma_i$ = 0.841 $V_{c,i}^{1/3}$. The collision integral for *i* in *air* ($\Omega_{i,air}$) was calculated as described by Bird and Stewart (Bird et al. 1960) using the Lennard-Jones parameter $\varepsilon_{i,air}$ which is the depth of the potential energy well for the molecule *i* in air. $\varepsilon$ is calculated from the melting temperature ($T_m$) as $\varepsilon_i$ = 1.92 $T_m$ (Bird et al. 1960). $\varepsilon_{i,air}$ and $\sigma_{i,air}$ was calculated as described in Equation 2.6 and 2.7, using $\sigma_{air}$ = 3.617 Å and $\varepsilon_{air}$ = 97 K.

$$\sigma_{i,air}=\frac{\sigma_{i,i}+\sigma_{air}}{2} \quad 2.6$$

$$\varepsilon_{i,air}=\sqrt{\varepsilon_{ii}\times\varepsilon_{air}} \quad 2.7$$

The integrated form of Equation 2.2 displayed in Equation 2.8 was used to calculate the saturation vapour pressure ($p^0$) at each temperature.

$$p^0 = -\frac{\rho_i RT}{4D_{i,air}\Delta t M_i}\int_{Dp,i}^{Dp,f}\frac{D_p}{f(Kn_i,\alpha)}\exp\left(\frac{-4\gamma_i M_i}{D_p\rho_i RT}\right)dD_p \qquad 2.8$$

In Equation 2.8 $D_{p,i}$ is the initial and $D_{p,f}$ is the final particle diameter, after evaporation. $\Delta t$ is the evaporation time corrected for the temperature effect on the volume flow rate in the VTDMA. Using Equation 2.9 and the assumptions above $p^0$ of a compound was calculated for an extended temperature range using the evaporation rate. Assuming that the enthalpy of evaporation was constant over the whole temperature range the Clausius-Clapeyron relationship (Equation 2.9) was used to calculate the enthalpy of evaporation ($\Delta H_{evap}$) and the $p^0$ at 298 K was inferred using extrapolation.

$$\frac{d\ln p^\circ}{d\left(\frac{1}{T}\right)} = -\frac{\Delta H^0}{R} \qquad 2.9$$

.

Since the method described here utilises the dynamic evaporation that takes place under non-equilibrated conditions the determination of the evaporation time is critical. The volumetric flow is corrected for the expansion of the air during heating.

## 2.3 Flow profile

With a fully developed laminar flow in a tube the gas flows in laminas without internally mixing with a velocity profile that is symmetric around the axis of the pipe, with the highest flow rates in the centre of the tube ($u_{max}$) and a flow rate close to zero closets to the walls. The dimensionless Reynolds number (Re), defined in Equation 2.10 is often used to understand fluid dynamics (Hinds 1999).

$$\mathrm{Re} = \frac{\rho V d}{\eta} \approx 6.6 V d \qquad 2.10$$

Where $\rho$ is the density of the gas, $V$ is the velocity, $d$ the pipe diameter and $\eta$ is the viscosity.

A flow in a pipe is considered to be laminar at Re < 2000. The mean flow rate $u_{mean}$ in a tube is calculated as described in equation 2.11

$$u_{mean} = \frac{Q}{A} \qquad 2.11$$

where $Q$ is the volumetric flow rate ($m^3\ s^{-1}$) and $A$ is the cross-section area ($m^2$).

In the laminar flow profile $u_{mean}$ is half the magnitude of $u_{max}$ and the velocity profile is described as in Equation 2.12

$$\frac{u}{u_{max}} = 1 - \left(\frac{r}{R}\right)^2 \qquad 2.12$$

where $u$ is the velocity at distance $r$ from the tube wall and $R$ is the tube radius. Figure 7 illustrates the velocity distribution of a fully developed laminar flow profile in a 6 mm i.d. tube as a function of the distance from the centre of the tube.

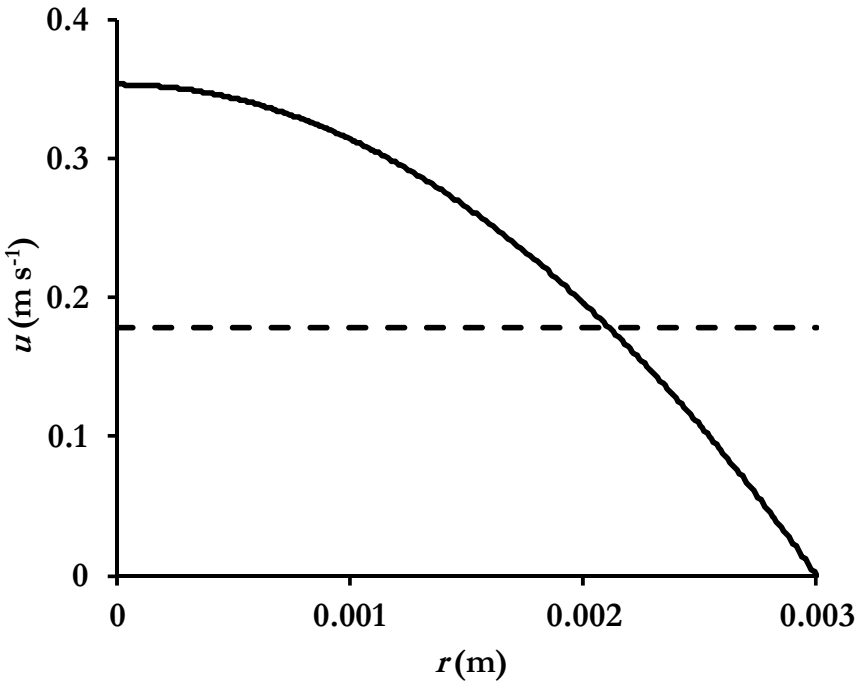


**Figure 7** The flowrate $u$ as a function of radius $r$ from the centre of a tube with 6 mm i.d. (solid black line) and the mean flow rate $u_{mean}$ (dotted black line).

The calculated flowrates (velocities) are used to calculate the evaporation time in the VTDMA system. In Paper I the mean flow i.e. plug flow rate was used to calculate the evaporation time. In order to better evaluate and understand the evaporation, the laminar flow profile was used to calculate the residence time in Paper II. The parabolic velocity profile was also used to calculate the reaction time in G-FROST (Paper IV) (Jonsson 2008).

# 3. Experimental

## 3.1 Equipment and techniques

### 3.1.1 Differential Mobility Analyser (DMA)

The differential mobility analyser (DMA) is a commonly used instrument to measure aerosol size distributions. It uses the size dependence of the mobility of charged particles in an electrical field. In Figure 8 the working principles of a DMA is seen. A polydisperse sample aerosol enters the system through a neutraliser to achieve a known both positive and negative charge distribution (Fuchs 1963). The neutralised aerosol then enters a cylinder with a charged rod in the centre. In the laminar flow the particles with the opposite charge according to the rod will be dragged towards the centre. The drag force the particles are subjected to is proportional to the diameter and shape of the particles. Small particles will impact on the charged rod and large particles will follow the sheath air flow out of the cylinder. Particles with an aerodynamic diameter corresponding to the set voltage will pass through the sample slit and form a monodisperse aerosol flow.

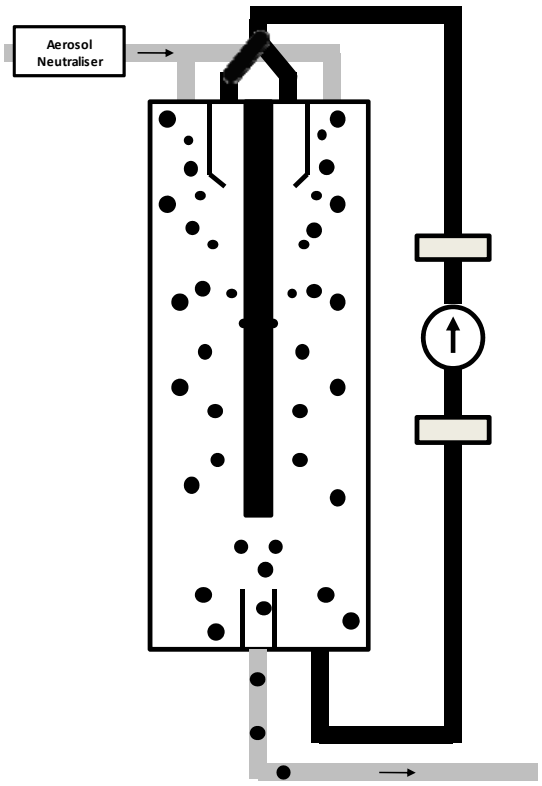


**Figure 8** A simplified view of a differential mobility analyser (DMA).

### 3.1.2 Condensation Particle Counter (CPC)

Nanosized aerosol particles are generally too small to be detected optically and in order to detect these particles a condensation particle counter (CPC) was used. In the CPC the aerosol flow is passed through a volume saturated with a working fluid, often water or alcohol (in this work 1- butanol was used) and thereafter passed through a cooled volume. When cooled down the working fluid will reach supersaturation and hence condense on the particles as the name "condensation particle counter" implies. The particles will grow and become detectable with optical methods. If the set voltage of the DMA is scanned and the particles counted with a CPC a full number and size distribution can be achieved with a time resolution down to 60 s. Set together in a unit the DMA and CPS make up the working parts in a scanning mobility particle sizer (SMPS) system.

### 3.1.3 Volatility Tandem DMA (VTDMA)

The main instrumentation used in the work to characterise aerosol particles was a Volatility Tandem DMA (VTDMA). With a VTDMA it is possible to first size select a close to monodisperse sample of an aerosol. This selected sample is then heated and the evaporated mass is finally quantified by observing the decrease in particle peak mode diameter. The VTDMA system consists of three main parts: *DMA 1*, an *oven* and an *SMPS* system. In DMA 1 a monodisperse aerosol is selected. The close to monodisperse aerosol is passed through the oven unit where the aerosol is heated to the desired temperature, and the evaporated gases are adsorbed by charcoal denuders.

A typical sample flowrate through this tube was 0.3 SLPM at 298 K. Assuming a "heated length" of 50 cm the mean velocity results in a residence time of 2.8 s in the heated part. The residence time is corrected for the change in volume flow with temperature using the ideal gas law. However under these flow conditions, Re is 90 and flows though pipes are considered to be laminar when Re < 2000 (Hinds 1999). The low Re in this system indicates a fully developed laminar flow profile with a max flow rate two times the mean flow. When the flow rate is calculated assuming a parabolic flow the median residence for a particle time is ~ 1.8 s.

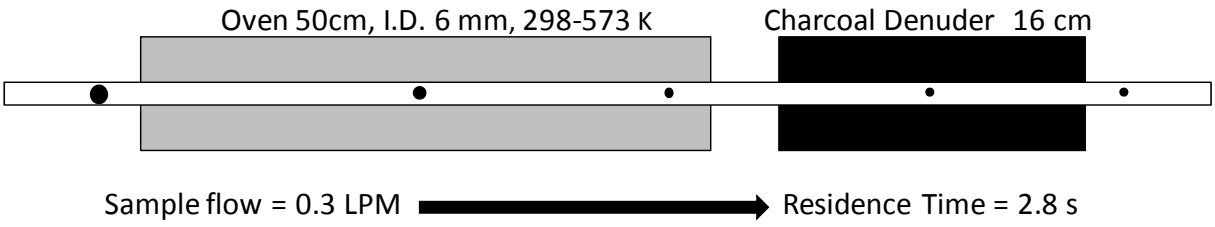


**Figure 9** A schematic of one of the ovens in the VTDMA system.

As illustrated in Figure 9 the heated part in the VTDMA consists of a 50 cm long stainless steel tube with an i.d. of 6 mm mounted in an aluminium block in order to avoid any temperature gradients and provide a temperature variability of ± 0.1 K. In all calculations it is assumed that the temperature of the aerosol is the same as the set temperature and that the contribution from the latent heat is negligible. In order to remove evaporated material a 16 cm long denuder loaded

with activated charcoal was used after the oven. Eight of these heating units are mounted in parallel to enable swift changes between temperatures with enough time for each unit to equilibrate at the set temperature. with enough time for each unit to equilibrate at the set temperature. One of these heating units was used as reference at a constant temperature (298 K). Finally the modified aerosol enters the SMPS system where the final particle diameter ($D_{pf}$) is determined. Besides the use in the calculation of the saturation vapour pressure, $D_{pf}$ is normalised to the initial particle diameter measured after the reference unit, ($D_{pi}$) and the volume fraction remaining ($VFR$) can be calculated as displayed in Equation 3.1.

$$VFR = \left( \frac{D_{pf}}{D_{pi}} \right)^3 \qquad 3.1$$

When the temperature dependence of VFR is plotted over an extended temperature range a so called thermogram is generated. A more volatile particle will evaporate more during the residence time in the VTDMA providing a smaller $D_{pf}$ and thereby a lower VFR (Equation 3.1).

In a VTDMA system with a relatively short residence time like the one used in this work the evaporation of the particles take place under non-equilibrium conditions meaning that the particle evaporates continuously during the residence time in the heated part of the oven. The evaporation time is then essential in any calculation of vapour pressure and enthalpy of vaporisation. An example of this is given in Paper I, (Figure 4) where thermograms for suberic acid aerosol at mean residence times from 1.1 to 4.5 s are displayed. In (Figure 5) in the same paper the calculated vapour pressures for the corresponding temperatures are given showing that no significant difference in vapour pressure for the different residence times were obtained.

## 3.2 Aerosol generation

### 3.2.1 Nebuliser

To generate sample aerosols from aqueous solutions of the pure compounds described in Paper I and II a nebuliser (TSI 3076 constant output atomizer) was used. This is a collision-type nebuliser that generates aerosols of constant particle size in concentrations over $10^7$ particles $cm^{-3}$. The nebuliser was operated in a non-circulating mode and fed with purified particle free pressurised air. The pure compounds were dissolved in deionised water (Milli-Q-plus) and delivered to the nebuliser using a peristaltic pump. The generated aerosol was dried with silica diffusion dryers and when needed, diluted to suitable concentrations before entering DMA 1. This method generates an aerosol with RH < 5% at room temperature. Aerosol particles created with this method can be solid (crystallised) or liquid (supersaturated droplets) depending on the purity of the sample but also by its physical properties like hygroscopicity, solubility or crystallisation rate (Mikhailov et al. 2009; Sjögren et al. 2007)

### 3.2.2 Smog chambers

In this work, SOA characterisation experiments were performed in three smog chambers. The AIDA chamber (Aerosols In a Dynamic Atmosphere), the SAPHIR chamber (Simulating Atmospheric Photochemistry In a large Reaction chamber) and the EUPHORE chamber (European PHOto chemical REactor). The AIDA and the SAPHIR chambers were used to investigate the OH induced ageing of SOA from the ozonolysis of limonene and α-pinene as described in Paper III and IV. The EUPHORE chamber was used to investigate the properties of aerosols formed during amine degradation in the atmosphere. This work was performed in association with the ADA-2010 (Amine Degradation in the Atmosphere) and was published in the final report of this project (Nielsen et al. 2010).

The AIDA chamber is an aluminium chamber hosted by the Karlsruhe Institute of Technology (KIT) in Karlsruhe, Germany. It has a volume of 84.5 $m^3$ and an inner surface area of 103 $m^2$. This large chamber is suited for investigating chemical kinetics, aerosol chemistry, aerosol physics and cloud microphysics. The whole chamber is located in a temperature controlled housing operated at temperatures from 183 K to 333 K, pressures from 1 to 1000 hPa and relative humidity from almost 0% to 100%. The chamber was equipped with a large suit of instrumentation as illustrated in Figure 10. The OH radicals were generated by the ozonolysis of a small symmetric alkene, tertramethyletylene (TME) in the dark (Lambe et al. 2007). This reaction generates OH radicals with a yield close to unity without any formation of condensable products. Experiments were performed at 273, 293, and 313 K using limonene and α-pinene as SOA precursors.

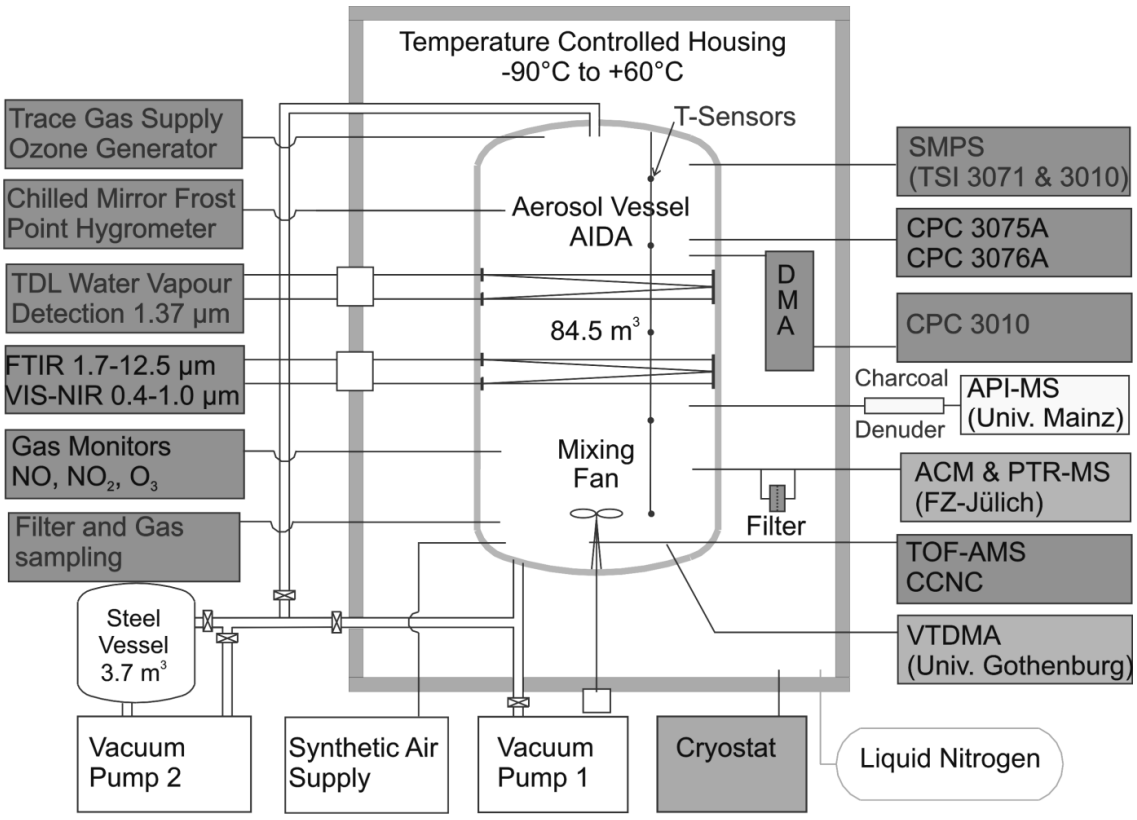


**Figure 10** A schematic of the AIDA chamber facility together with additional instrumentation.

The SAPHIR chamber is a 270 $m^3$ double walled fluorinated ethylene propylene (FEP) outdoor photoreactor suitable for OH production using natural sunlight, e.g. photolysis of $O_3$, HONO or $H_2O_2$. It is hosted by the FZK (Forchungszentrum Jülich). This chamber facility has been used for low concentration experiments to increase the understanding of photochemical processes in the troposphere (Rohrer et al. 2004) and recently also been used for aerosol formation studies (Rollins et al. 2009). It enabled studying SOA ageing under close to atmospheric conditions. The roof is closable to control the actinic flux. In the SAPHIR, the OH radicals were generated by natural sunlight induced photolysis of ozone in the presence of water and using α-pinene as precursor at ambient temperatures (293 to 296 K). In general the experiments in the AIDA and SAPHIR were outlined as follow. The experiment was initiated with the addition of ozone to the conditioned and humidified chamber. After characterisation of the background conditions, limonene or α-pinene was added as SOA precursors and the SOA formation started instantaneously. Within an hour the precursor was consumed and a stable aerosol was formed and the ageing part of the experiment was initiated i.e. exposure to OH radicals.

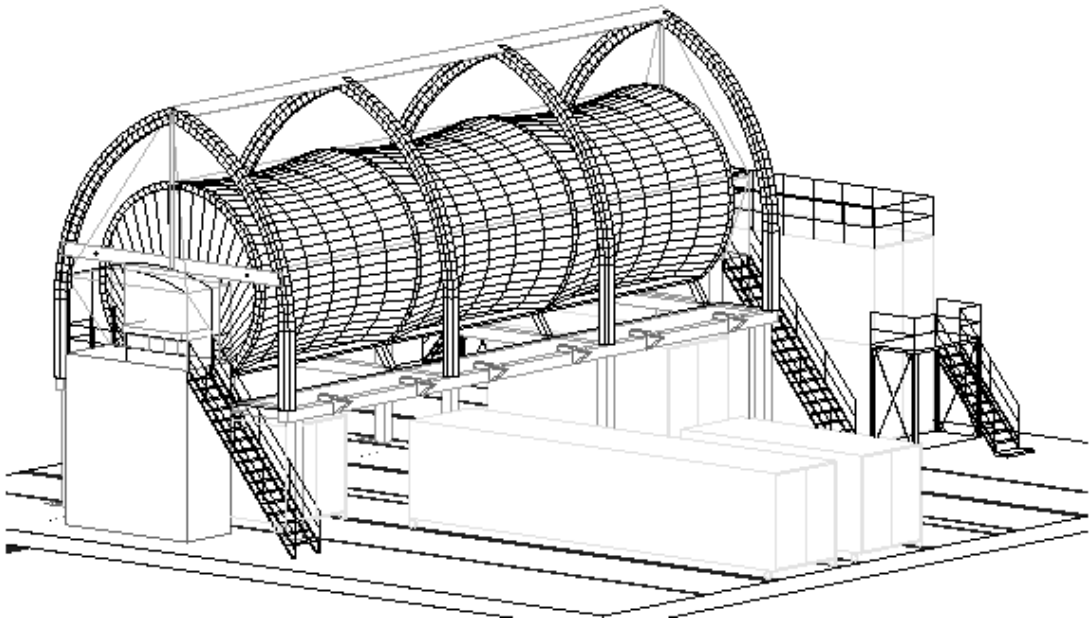

**Figure 11** A schematic of the SAPHIR chamber.

The European PHOto chemical REactor (EUPHORE) consists of two 200 $m^3$ hemispherical Teflon chambers designed for photochemical studies. The chambers are protected by steel canopies, which are opened during the photooxodation experiments. The chamber is hosted by La Fundación CEntro de Estudios Ambientales del Mediterráneo (CEAM), Valencia, Spain. In a similar way as in the SAPHIR chamber, natural sunlight is used to induce photo chemical reactions. Experiments were performed using monomethylamine, dimethylamine and trimethylamine under low (10 ppb) and high (100 ppb) $NO_x$ conditions. A typical EUPHORE experiment started whit the addition of precursors and reagents to the preconditioned chamber. Some background formation of aerosol particles was generally observed, but these background

particles were considered to be negligible and to consist of aminium nitrate particles from the precursor amine and $HNO_3$ present in the chamber as a contamination from the $NO_2$ addition. The canopy of the chamber was opened after the reagents were considered to be well-mixed, and the aerosol formation started. The aerosol was characterised with VTDMA and AMS. Some experiments lasted up to 12 hours with repeated measurements of both gaseous and condensed phase.

### 3.2.3 Laminar flow reactor

The Gothenburg Flow Reactor for Oxidation Studies at low Temperatures (G-FROST) is a laminar flow reactor vertically mounted in a temperature controlled housing. This reactor has recently been used to examine the oxidation mechanisms of BVOCs with ozone including the dependence of OH radicals, relative humidity (RH) and temperature (Jonsson et al. 2006; Jonsson et al. 2008a; Jonsson et al. 2008b). It consists of a 191 cm long glass tube with an inner diameter of 10 cm. In order to reduce interactions between the walls and reactive gases the inside is coated with halocarbon wax. The precursor gas and any other reactants e.g. OH-scavenger or water is introduced via the bulk-flow into the reactor. The ozone is introduced into the reactor via a movable mixing unit. To further reduce gas and particle interaction with the walls, the flow reactor is operated under laminar flow conditions ($Re < 2000$) and only the centre part of the flow is sampled via a sampling funnel. The reaction time is depending on position of the mixing unit, mass flow rate, temperature and pressure and is calculated from the mean velocity of the fraction of the centre flow that is extracted via the sampling funnel. The mass flow rate, temperature and pressure all have very little variation once set and provided a fixed reaction time. The reaction temperature can be controlled within $\pm$ 0.1 K and set between 243 and 323 K. A well defined RH ($\pm$ 0.1%) was achieved by passing purified air flowed through a Gore-Tex tube submerged in temperature controlled deionised water. The desired RH of the air flow was set by the water temperature. The humidity in the system was monitored by a dew point meter (Optidew, cooled mirror dewpoint meter, dewpoint $\pm$ 0.2 K, gas temperature $\pm$ 0.1 K, Michell Instruments Ltd.) and a relative humidity meter (HMP143A, Vaisala). The organic precursor limonene was introduced to the flow reactor by letting a flow of nitrogen pass over a temperature controlled diffusion vial. The 2-butanol used as OH-scavenger was distributed in a similar way with the difference that the $N_2$ flow, to be able to reach sufficient concentrations, was bubbled through the liquid reagent and thus not diffusion limited. Ozone was produced using pure oxygen passing through a commercial UV-ozone generator (UVP, OG-3, SOG), and monitored using an ozone analyser (Thermo Environmental Instruments 49C Ozone analyser). In order to avoid long ozone residence times in the tubing, $N_2$ was used as a make-up gas to increase the flow after the UV-ozone generator and into the reactor. After changing any experimental conditions the SOA production was stabilised during 2 – 3 hours before any characterisation took place. The organic concentrations were determined off-line before and after an experimental series. All organics were prior to analysis sampled from the flow reactor using adsorbent tubes (Tenax-TA). The samples were desorbed using thermal desorption (Unity I, Markes International Ltd.) and analysed with gas chromatography and flame ionisation detection (Finnigan/Tremetrics 9001, GC-FID). A schematic of the working principles of the G-FROST facility and its instrumentation is seen in Figure 12.

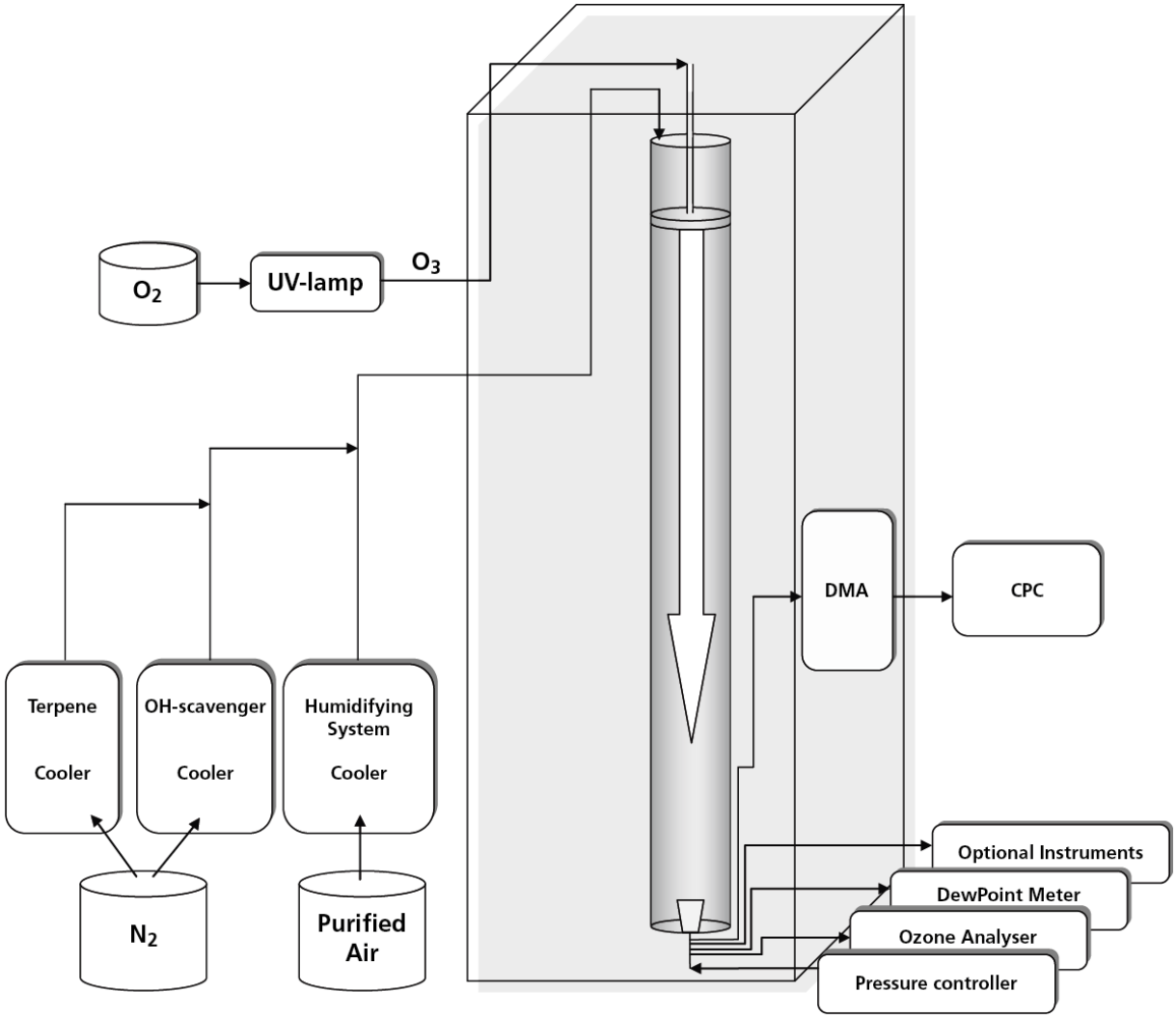


**Figure 12** Schematic of the G-FROST facility illustrating how precursor, OH-scavenger and water were delivered to the top of the reactor and ozone was introduced via the mixing unit.

The experiments in G-FROST presented in Paper V was designed to investigate the effects of ozone concentration and associated radical chemistry on the volatility of SOA from limonene ozonolysis with or without the use of OH scavenger (2-butanol). The experiments were performed at 298 K and in all except for one dry (5%) experiment at a relative humidity of (40%). Four different ozone concentrations (600, 2000, 3500 and 5000 ppb) were tested using a reaction time of 238 s. The 2-butanol was in selected experiments added in order to remove OH radicals formed in the ozonolysis reaction with the precursor and to have ozone as the only initiating oxidant. However, it is important to consider that the addition of the scavenger is also influencing other radical concentrations in the system. The products from the OH radical reaction with 2-butanol are 2-butanone and the radicals $RO_2$ and $HO_2$ that may take part in the secondary chemistry. The effect of different OH-scavengers with regards to produced SOA number and mass has been further investigated by Jonsson et al. (2008a). In this work the

VTDMA system was applied with the aim to elucidate how chemistry influenced the volatility of the produced SOA. In order to further evaluate the experimental results, simulations were performed using the kinetic chemical model developed by the Kamens group of University of North Carolina (Li et al. 2007).

### 3.2.4 Summary and comparison

In this study several different methods were applied to study the formation and ageing processes of SOA (Table 2). The advantage of chamber studies is the possibly to study long time processes e.g. up to several days. Although results from these long time studies must be corrected for several different reasons. Teflon walls have an uptake of SOA particles and interact in equilibrium with the SOA gas phase especially with SVOC and amines, which has to be considered and corrected for when estimating e.g. SOA yield (Matsunaga et al. 2010). Teflon is also slightly permeable so in order to maintain the chamber volume a continuous inflow of air is necessary leading to dilution. Aluminium walls on the other hand do not interact with particles in the same way, but have a larger irreversible uptake of certain polar SVOCs e.g. dicarboxylic acids that needs to be characterised and accounted for. Outdoor chambers also have the possibilities to use natural sunlight to study photochemistry but they only operate at ambient temperature conditions. With the AIDA chamber and G-FROST it is possible to perform experiments at a well defined wide temperature range. The main advantages with G-FROST are the possibility to generate a continuous flow of SOA with a fixed reaction time for hours and over a wide experimental temperature and humidity ranges. In Paper V that describes the MUCHACHAS further advantages of using multiple infrastructures are highlighted.

**Table 2** Comparison of the infrastructures used in this thesis for SOA studies.

| Infra-structure | Technique | Temperature range (K) | Main sinks | Time |
|---|---|---|---|---|
| **G-FROST** | Laminar Flow Reactor | 243-323 | Diffusion | Minutes |
| **AIDA** | Aluminium Chamber | 183-333 | Gas to the walls | Days |
| **SAPHIR** | Teflon Chamber | Ambient | Particles/gas to the walls, dilution | Days |
| **EUOPHORE** | Teflon Chamber | Ambient | Particles/gas to the walls, dilution | Days |

## 3.3 Additional Instruments

The time-of-flight aerosol mass spectrometer (TOF-AMS. Aerodyne Inc.) is an instrument that allows real-time and in situ analysis of fine and ultrafine particles. The working principles of the AMS are explained in detail in Jayne et al. (2000) and DeCarlo et al. (2006). The instrument measures the size distribution and chemical composition of particles between 0.03 to 1 μm with a

time resolution of 60 s. The particles are sampled through a critical orifice (diameter 100 μm) with a sample flow of 80 $cm^3$ $min^{-1}$ and focused by an aerodynamic lens that removes all particles larger than 1 μm in diameter. After the lens the focused particle beam is accelerated when entering a vacuum chamber where a mechanical chopper allows a packet of particles (beam chopped) to be accelerated according to their vacuum aerodynamic diameter ($D_{va}$) and thereby giving size distribution data. The particles then enters the vaporisation-ionisation chamber where the non-refractory components of the particles are flash-vaporised on a hot surface (~600 °C) and ionised by electron impact (e.g. at 70 eV). The resulting positively charged ions are guided into the time of flight-mass spectrometer (TOF-MS). The collected mass spectra (m/z from 4 to 350 in a minute scale) give information on the chemical composition. The relatively high fragmentation does not allow for molecular identification, but provides organic mass, extent of oxidation and ratios between organic and inorganic composition. In addition, the particle diameter measured in vacuum $D_{va}$ is related to the particle mobility diameter measured at atmospheric pressure with the SMPS through the particle density (ρ), this is described in Paper II and was used to calculate the density for the aminium nitrates investigated and presented in (Table 1), Paper II.

An instrument that gives more detailed information of the chemical composition of the aerosol particles is the atmospheric pressure chemical ionisation-mass spectrometer (APCI-MS). The APCI-MS was used to identify three selected aerosol constituents (pinic, pinonic and a tricarboxylic acid) in the AIDA experiments. The technique is described in detailed by Müller et al. (2011). In short, the aerosol is sampled through a charcoal denuder in order to remove gaseous components and the residual particles are directly introduced into a modified APCI source. With the use of this relatively soft ionisation method the selected acids form stable molecular ions and can be identified with the use of reference compounds and on-line MS/MS technique.

In order to monitor the gas phase aerosol components the PTR-MS technique (IONICON, Innsbruck, Austria) was utilised in the experiments performed in the AIDA, SAPHIR and EUPHORE chambers. The PTR-MS is described in detailed by Jordan et al. (2009), Lindinger et al. (1998), Nielsen et al. (2010) and in Paper III-IV. Shortly, the PTR-MS draws the aerosol sample through a Teflon filter and uses $H_3O^+$ or $NH_4^+$ to ionise the analyte gases via proton transfer reaction and analyses the molecular ions with MS-technique. The PTR-MS is an excellent instrument to on-line follow the temporal behaviour of specific organic trace compounds.

# 4. Results and Discussion

The emphasis of this work was on increasing the knowledge of thermal and physical properties of SOA and its constituents. Paper I and II present data on the saturation vapour pressures ($p^0$) and enthalpies of evaporation ($\Delta H$) of pure ubiquitous SOA constituents. Seven straight chain dicarboxylic acids, pinic and pinonic acid are presented in Paper I while ammonium nitrate and four alkylaminium and ethanolaminium nitrate salts are presented in Paper II. Paper III and IV describe the results from the multiple chamber chemical ageing study (MUCHACHAS) where the VTDMA was used to study OH radical ageing of SOA generated from ozonolysis using limonene and α-pinene as precursors in large smog chamber facilities. Paper V describes the thermal properties of limonene SOA at different ozone levels in the G-FROST facility. In order to put the data on the aminium nitrates published in Paper II in perspective the thermal properties of SOA formed from selected amines are presented herein. These experiments were performed during the Amine Degradation in the Atmosphere (ADA-2010) campaign and are published in the final report of that project (Nielsen et al. 2010).

## 4.1 Vapour pressures of SOA constituents

Some key features to understand the fate and behaviour of the atmospheric oxidation products that make up the SOA mass are the saturation vapour pressures and enthalpies of vaporisation. Sound knowledge of these properties for single compounds can increase the understanding of the properties of the complex mixture that is SOA. In this work the thermal properties of suspended nanosized particles generated from nebulised aqueous solutions of 15 compounds, all being known aerosol constituents, were tested. The resulting values for $\Delta H_{sub/vap}$ and $p^0_{(298\ K)}$ of these compounds are displayed in Table 3.

**Table 3** Calculated saturation vapour pressures and enthalpies of sublimation as published in Paper I and II.

## Carboxylic acids

| Name | $p^0$(298 K) ($10^{-5}$ Pa)¤ | $\Delta H_{sub}$(kJ mol$^{-1}$) T (K)# |
|---|---|---|
| **Succinic acid** | $6.4^{+2,0}_{-1,8}$ | 112 ± 12 (303-328) |
| **Glutaric acid** | $85^{+31}_{-22}$ | 101 ± 20 (298-318) |
| **Adipic acid** | $5.8^{+1,8}_{-1,4}$ | 97 ± 8 (303-333) |
| **Pimelic acid** | $17^{+8.0}_{-5.0}$ | 127 ± 20* ( 301-323) |
| | $1.8^{+6.0}_{-1.3}$ | 161 ± 50 (310-327) |
| **Suberic acid** | $1.4^{+0.6}_{-0.4}$ | 101 ± 10 (303-357) |
| **Azelaic acid** | $4.7^{+0.8}_{-0.7}$ | 96 ± 5 (303-343) |
| **Sebacic acid** | $0.9^{+0.5}_{-0.4}$ | 100 ± 12 (308-363) |
| **Pinonic acid** | $0.42^{+0.2}_{-0.1}$ | 90 ± 7 (318-358) |
| **Pinic acid** | $10^{+1.5}_{-1.8}$ | 83 ± 5* (303-326) |

## Aminium nitrates

| Name | $p^0$(298 K) ($10^{-4}$ Pa) ¤ | $\Delta H_{sub}$(kJ mol$^{-1}$) T (K) # |
|---|---|---|
| **Ammonium nitrate** | $6.79^{+2.2}_{-1.7}$ | 72 ± 5.3* (309 – 330 K) |
| **Methylaminium nitrate** | $2.88^{+0.6}_{-0.5}$ | 65 ± 2.3* (318 – 345 K) |
| **Dimethylaminium nitrate** | $3.92^{+1.2}_{-0.9}$ | 63 ± 3.9* (315 – 339 K) |
| **Trimethylaminium nitrate** | $5.37^{+1.1}_{-0.9}$ | 66 ± 3.2* (308 – 333 K) |
| **Ethylaminium nitrate** | $2.68^{+14}_{-2.2}$ | 54 ± 18* (323 – 343 K) |
| **Ethanolaminium nitrate** | $0.89^{+0.4}_{-0.3}$ | 74 ± 3.9* (330 – 348 K) |

¤Extrapolated to 298 K, #Calculated for the given temperature intervals,
*Enthalpy of vaporisation.

There are a number of reported values for the saturation vapour pressures and enthalpies of vaporisation of straight chain dicarboxylic acids in the literature, often with quite large discrepancies e.g. reported literature values for the solid state vapour pressures of pimelic acid ($C_7$) ranges from $9.7 \times 10^{-7}$ Pa (Bilde et al. 2003) to $7.2 \times 10^{-5}$ Pa (Saleh et al. 2008). The differences in reported values are somewhat depending on which method that has been used. These methods are described in more detail in Paper I and II.

In addition, several theoretical methods to estimate these properties are available. In an extensive study of several vapour pressure estimation models performed by Barley et al. (2010) some difficulties with these models were pointed out. These estimation models are often based on empirically group contribution methods generated from large databases with vapour pressures. However, the empirically data for low volatile compounds containing multiple functional groups, like SOA constituents, are scarce. In addition, these methods have large difficulties to handle ionic compounds, i.e. salts like aminium nitrates. Barley et al. (2010) also found that even moderate errors in vapour pressures generated large differences in the amount of aerosol formed when used in SOA predicting models and therefore the use of reliable experimental methods are necessary.

#### 4.1.1 Dicarboxylic acids

In Paper I the calculated $\Delta H_{sub}$ for the $C_4$ to $C_{10}$ straight chain dicarboxylic acids ranged from 96 to 161 kJ $mol^{-1}$ and the saturation vapour pressures extrapolated to 298 K ranged from $10^{-6}$ to $10^{-4}$ Pa. As seen in Paper I, these values agree quite well with literature data. An additional interesting feature of the straight chain dicarboxylic acids is the melting point alternation with the number of carbon atoms, see Thalladi et al. (2000) and references therein. The explanation for this phenomenon is the stronger bonds in the crystalline state for the even numbered acids. The vapour pressures and enthalpies of sublimation presented in Paper I showed no significant odd-even alternation behaviour. The reason for this is probably connected to the phase of the generated aerosol particles. In the work by Bilde et al. (2003), studying the solid state properties of dicarboxylic acid nanoparticles, the alternation with carbon number was observed in both the saturation vapour pressures and the enthalpies of sublimation measured whereas in the work by Koponen et al. (2007), using supersaturated droplets, this alternation was not seen. The difference in evaporation from liquid and crystalline phases was demonstrated in the case of pimelic acid ($C_7$) in Paper I (Figure 8). Pimelic acid showed a significant bimodal behaviour when heated to 310 K. This was explained by evaporation from an externally mixed aerosol consisting of both liquid and crystalline particles, evidently both phases co-exist. The enthalpies of sublimation and evaporation were calculated for both phases and the difference (~34 kJ $mol^{-1}$) corresponds quite well with the literature value for the enthalpy of fusion (Burger et al. 1996) as reported in Paper I. Similar observations were done by Chattopadhyay et al. (2005) studying evaporation from odd numbered dicarboxcylic acids ($C_5$, $C_7$, $C_9$).

During the work with aerosol generated from nebulised aqueous solutions of pinonic acid it became evident that impurities can have large effects on the obtained results. The initial experiments were not reproducible and had non-volatile evaporation residues ranging from 5 to 10% in VFR. In comparison, none of the other examined compounds had more than 2% residue. Two different bulk samples of the commercially available acid were tested (Aldrich, 98%),

producing the same results. A pinonic acid sample, purified by recrystallisation produced a totally different thermal behaviour with a residual VFR < 1%. The resulting thermograms are illustrated in Paper I, (Figure 10). Problems with impurities in commercial samples of pinonic acid have been reported earlier in the study by Bilde and Pandis (2001). This result implies that part of the large experimental uncertainties in the literature might be associated to the purity of the sample. Impurities in an aqueous sample can disturb the crystal structure and hinder the efflorescence process when the particles are dried. However, atmospheric particles do not consist of only one dicarboxylic acid. Instead evaporation and partitioning from particles with complex mixtures of organic and inorganic compounds are relevant for the atmosphere. The results in the experiments described above and in Paper I have shown that the phase and the composition of the evaporating particle are important and reflected in its thermal behaviour.

#### 4.1.2 Ammonium and aminium nitrates

The vapour pressures and enthalpies of vaporisation of nitrate salts of ammonia, four alkylamines and monoethanolamine (MEA), were obtained in a similar way as described for the dicarboxylic acids. Except for ammonium nitrate, no earlier data on these properties were found in the literature.

The precursor amines used herein are all volatile compounds with vapour pressures ranging from 145 to 351 kPa and in the atmosphere they will be found in the gaseous phase. Their physical and chemical properties are similar as is seen in Paper II (Table 4). The similar properties of the precursor amines are reflected in the resulting measured properties of the corresponding nitrate salts. The vapour pressures of these compounds range from $10^{-5}$ to $10^{-4}$ Pa and the enthalpies of evaporation from 54 to 72 kJ $mol^{-1}$. Their saturation vapour pressures are about one order of magnitude higher than for the dicarboxylic acids as is seen in Table 3 but still low enough to form SOA via its formation from the reaction of the parent amine with $HNO_3$ (Smith et al. 2010). The lowest saturation vapour pressure measured in these experiments was for MEA-nitrate; with almost a tenfold lower pressure than the alkyl aminium nitrates and more similar to the dicarboxylic acids. One important difference between dicarboxylic acids and aminium nitrates is the evaporation process. Most probably the dicarboxylic acids evaporate as molecules with a very small degree of decomposition under atmospheric conditions. Exactly how the evaporation process proceeds for salt particles is still unknown but probably the largest part evaporates via dissociation of the salt on the particle surface forming $HNO_3$ and the amine. In the work by Chien et al. (2010) studying vaporisation of ammonium nitrate from bulk samples, it became evident that possibly as much as 20% of ammonium nitrate evaporates without decomposition. However, this has not been studied for evaporation from aerosol particles or for aminium nitrates.

### 4.2 Volatility of SOA from monoterpenes

The characterisation of the thermal properties, i.e. the volatility of SOA provides indirect information that can be used to understand ongoing processes in the aerosol e.g. ageing. In order to understand these processes the VTDMA unit was utilised to characterise the thermal properties of SOA particles. In Papers III, IV and V several different effects on the volatility of SOA, generated from ozonolysis of monoterpenes (α-pinene and limonene) in both chamber and flow reactor experiments, were analysed.

As an example of typical data collected during the chamber SOA ageing experiments in AIDA and SAPHIR, an ozonolysis experiment from the AIDA (limonene, 293 K) is illustrated in Figure 13. In both chambers the nucleation and growth of the particles started instantly when the precursor was added to the ozone containing chamber at time equal to zero, as is seen in Figure 13. A sharp increase in the SOA mass and VFR (383 K) were then seen.

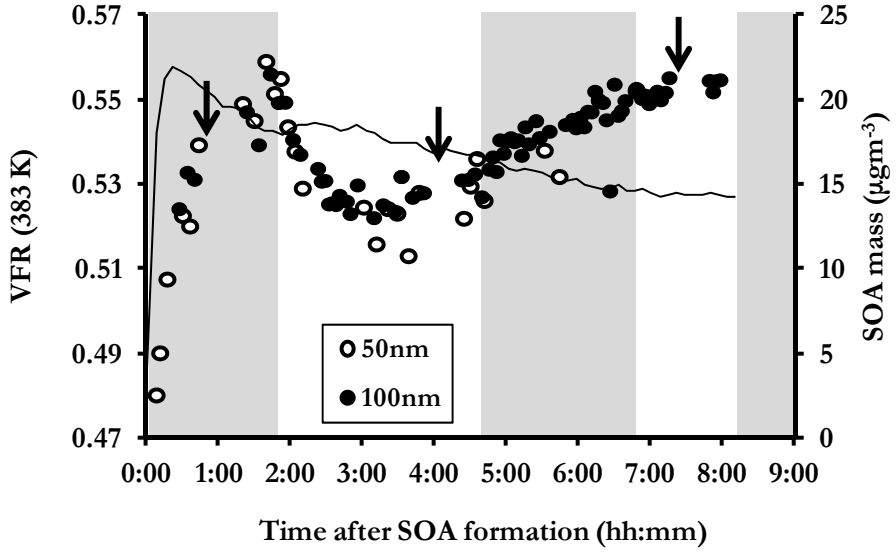


**Figure 13** (Paper III, Figure 1) Ozonolysis of limonene at 293 K, VFR (383 K) (filled and unfilled circles) and the SOA mass measured with SMPS (solid black line).

When all the precursor had reacted the aerosol mass concentration peaked and started to decrease due to dilution and wall interactions. The "stable" SOA was characterised in detail with the VTDMA system by recording thermograms at times marked with arrows in Figure 13. After 1-2 hours the "ageing part" of the experiment was initiated, and in the AIDA this was done by adding TME and in the SAPHIR the roof was opened (see section 3 Experimental or Paper III for a more detailed description). The "ageing part" is illustrated by the white areas in Figure 13. As a result of the increased OH radical concentration an increase in SOA mass and a decrease in VFR (383K) were observed. After one hour of OH radical exposure, the mass increase declines and the SOA mass starts to decrease. At the same time the decrease in VFR stops and the aerosol starts to get less volatile. Approximately four hours after the start of the experiment (~2 hours of OH-exposure) an additional VTDMA characterisation was performed. In some experiments a second OH radical exposure period was initiated. In the experiment displayed in Figure 13, this was done at approximately 7 hours after the start of the experiment. The AIDA experiments lasted from 8 to 24 hours. In SAPHIR the experiments was extended for up to three days.

#### 4.2.1 Ozonolysis

There is a clear difference in the thermal properties of the SOA formed from ozonolysis of α-pinene and limonene, where limonene SOA is less volatile than the SOA formed from

α-pinene. In Figure 14 thermograms, i.e. the VFR over an extended temperature range, of SOA formed from the ozonolysis of α-pinene and limonene under similar experimental conditions are compared. This difference in volatility is in line with the results shown by Jonsson et al. (2007). The fact that limonene SOA is less volatile can be linked to that oxidation products from limonene ozonolysis are efficient nucleating species (Jonsson et al. 2006) and as seen in previous work, different precursors also have different ability to form SOA, i.e. will have different yields (Saathoff et al. 2009).

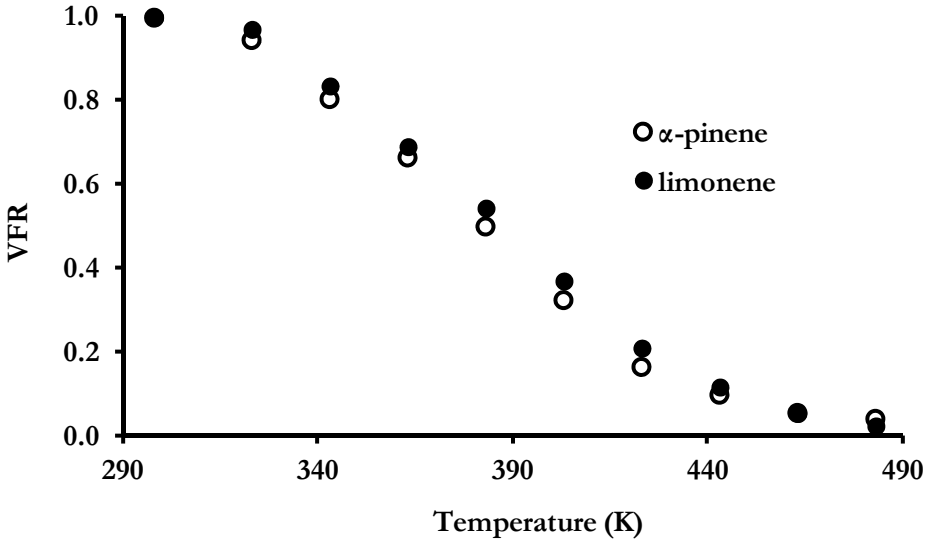


**Figure 14** Comparison of the temperature dependence of VFR for SOA formed from ozonolysis of limonene and α-pinene at 293 K in the AIDA chamber. Samples were taken 1-2 hours after the addition of ozone.

The volatility of the SOA produced in the AIDA chamber was not only dependent on which precursors that were used. In addition, the results from the experiments published in Paper III (Figure 6) showed that the reaction temperature has a large effect on the volatility of the formed particles, where a lower reaction temperature produced a more volatile SOA. The SOA experiments displayed in Paper III (Figure 6) were performed at 273, 293 and 313 K with the use of α-pinene as a precursor. A similar ozonolysis temperature effect on the volatility has been reported earlier by Jonsson et al. (2007) and this effect can be explained either as changes in chemistry or in the partitioning of SVOC. However, in order to avoid the effect of partitioning the VTDMA measurements were done on a sample aerosol that was equilibrated to room temperature in both this and the previous study. Now also for the first time simultaneous analysis of the particle chemical composition with APCI-MS were performed (Müller et al. 2011). The APCI-MS was used to track the relative contribution of some α-pinene oxidation products to the SOA mass in order to analyse if there is a chemistry effect. The products studied were pinonic acid, pinic acid and 3-methyl-1,2,3-butanetricarboxylic acid (MBTCA) and the results from this

analysis are displayed in Paper III (Figure 7). This Figure shows how the relative SOA contribution of the low-volatile MBTCA increased from 10 to 30% with increased reaction temperature. Müller et al. (2011) proposed that MBTCA is formed from the gas phase reaction of OH radicals with pinonic acid. As pinonic acid is an SVOC it will partition towards the gaseous phase with increased reaction temperature, hence being more susceptible for the OH radical reaction at higher reaction temperature. A similar ozonolysis-temperature effect on the volatility was seen in the limonene experiments, but no further analysis of the chemical composition of the particles were done in those experiments.

#### 4.2.2 OH-chemistry

As described in Figure 4 there are several processes involved in the atmospheric ageing of SOA. It is believed that OH radicals can take part in reactions on the surface of the particle by reactive uptake, a process that should increase the O/C and decrease the volatility of the particles but have a low influence on the condensed mass (George et al. 2010; Pöschl et al. 2007). If it is possible for the OH radicals to diffuse into the particle bulk, condensed phase reactions will occur. These could induce e.g. the formation of oligomers that would reduce the volatility but in the same way as for surface reactions it will not significantly contribute to the mass (Hallquist et al. 2009). Gaseous IVOC or SVOC SOA components can be subjected to OH radical reactions as shown in Figure 2. The products from these reactions can contribute to the SOA mass by condensational growth and thereby change the composition of the particles and their volatility (Robinson et al. 2007). During the experiments in both the AIDA and SAPHIRE chambers it was observed that the production of OH radicals by addition of TME or by photochemistry in presence of a fresh ozone initiated SOA (approximately 2 h after the addition of ozone) led to an increase in SOA mass, as is seen in Figure 13. The OH radical initiated oxidation of the gaseous ozonolysis products formed new condensable products that contributed to the SOA mass but did not induce any new particle formation. The new additional SOA mass made the particles more volatile. This increase in volatility was observed as a decrease in VFR (383 K), as is shown in Figure 13. The effect of the OH-exposure started to subside after one hour and the reason was anticipated to be that the reactive gaseous SVOC and IVOC compounds are consumed and hence the gaseous OH-chemistry "dies". For these experimental conditions it seems like the surface and condensed phase chemistry were too slow to be observed neither on the volatility nor on the SOA mass when turning off and on the radical OH-sources.

Another result demonstrating the importance of available reactive species in the gas phase in order to observe an effect of OH radical induced ageing was the effect of reaction temperature. The lower the experimental temperature used, the smaller was the observed decrease in VFR and increase in SOA mass when adding OH chemistry. This temperature dependence was observed in both α-pinene and limonene experiments and is illustrated for two limonene experiments in Paper III, (Figure 9). As the partitioning is strongly dependent on the temperature, reactive SVOC will partition into the condensed phase and be protected from the faster gas phase OH radical oxidation at the low temperature experiments (Donahue et al. 2006). In addition, it was noted that the mass of SOA had an effect where the ageing became less effective in high concentration experiments when the gas phase concentration of SVOC will be lower due to increased partitioning towards the condensed phase.

To further understand the processes behind the effect of OH radical ageing, one α-pinene experiment performed in the AIDA chamber was evaluated using the Computer SIMulation of Aerosols (COSIMA) model by Naumann (2003) and Saathoff et al. (2009). The COSIMA model simulates the condensed phase concentrations of four product proxies from the α-pinene oxidation. These four products are distinguishable by their vapour pressures, LVOC ($6.5 \times 10^{-6}$ Pa) formed in the ozonolysis, OH-product ($3 \times 10^{-5}$ Pa) which is a secondary product formed from the precursor and primary products, SVOC ($4.7 \times 10^{-4}$ Pa) formed in the ozonolysis and an IVOC product formed in the ozonolysis that will not partition into the condensed phase. In Figure 15 the time trends of the three condensable products are displayed and it is clearly seen how the fractions of the different proxies that contribute to the total SOA mass changes with time.

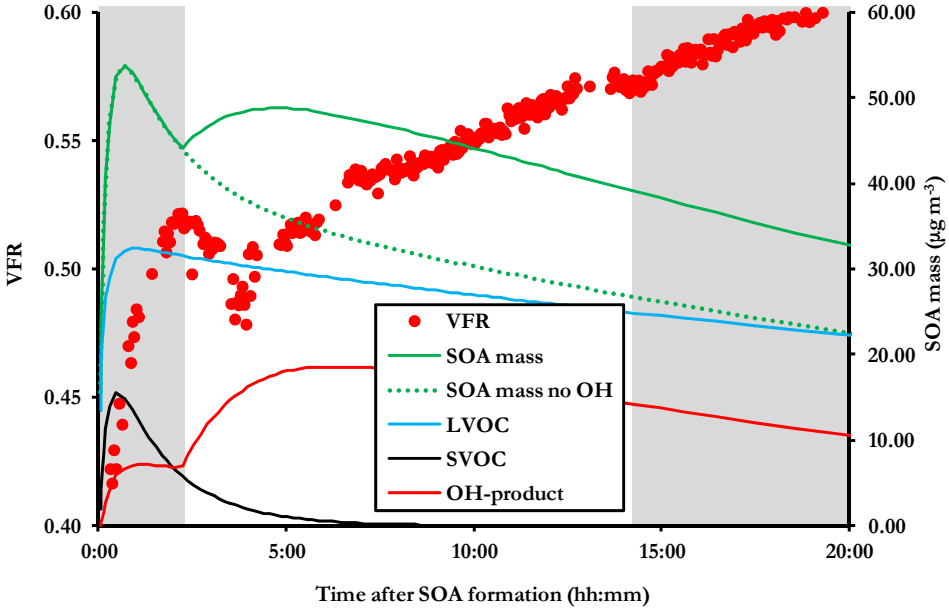


**Figure 15** (Paper III, Figure 4) Calculated particulate mass concentrations of three α-pinene oxidation products using the COSIMA model and VFR (383 K) as function of time after ozonolysis.

At the start of the experiment, the SVOC product was formed rapidly and partitioned into the condensed phase and together with the LVOC product contributed to the rapid increase in SOA mass. As soon as the α-pinene precursor was consumed, the SVOC product started to partition back into the gaseous phase and the concentration in the condensed phase decreased. The LVOC product was mainly formed from the ozonolysis and most of it was found in the condensed phase all through the experiment. The OH-product was formed in a small amount during the ozonolysis however most of it was formed after the onset of the OH radicals (TME addition). The increase in SOA mass was attributed to formation of the OH-product and its partitioning into the condensed phase. In a similar way as in the earlier described experiments the measured VFR (383 K) decreased initially when the OH-ageing was initiated, and this increase in volatility corresponds to the change in SOA composition. The relative amount of the compounds formed by OH radical chemistry increased and the LVOC decreased in the condensed phase. This change in composition resulted in a more volatile aerosol.

### 4.2.3 Flow reactor studies

The G-FROST setup was used together with the VTDMA system to investigate the volatility of SOA particles formed from the ozonolysis of limonene. The goal was to evaluate the effect of ozone and radical chemistry on the SOA formation and its volatility.

As described in section 1.2.2, alkenes e.g. limonene will react fast with both ozone and OH radicals in the atmosphere. Limonene is a so called diene having two double bonds, one endocyclic (within the ring structure) and one exocyclic (outside the ring structure). This gives limonene a higher reactivity with both ozone and OH radicals compared to alkenes with one double bond. The rate of the ozone reaction with the endocyclic double bond is approximately three times faster than with the exocyclic bond (Jiang et al. 2010). For the OH radical reaction the endocyclic is assumed to be favoured but reaction at both sites occurs (Calvert 2000) and in the Master Chemical Mechanism (MCM) the fractions are 1/3 exocyclic and 2/3 endocyclic for OH addition (http://mcm.leeds.ac.uk). The molecular structure of limonene generates possibilities for the formation of a wide array of oxidation products and in a similar way as for the SOA experiments described earlier in this thesis it is assumed that the yield of the different products formed is controlled by the reaction conditions. The chemical structures and estimated vapour pressures of 6 possible limonene oxidation products and for one experiment also their simulated relative contribution to the aerosol are given in Paper V (Table 2).

When the experimental results were evaluated it became clear that the ozone levels, RH and OH chemistry have impact on both the amount and properties of the SOA formed. It was demonstrated that higher amount of SOA formed was observed at elevated ozone concentration and in addition the formed SOA became less volatile. The reduced volatility is shown in Figure 16 as an increase in VFR for the SOA particles produced under elevated ozone concentrations. In the small insert in Figure 16 the number size distributions illustrates the enhanced nucleation with higher ozone concentrations as the number of particles increases with the ozone concentration and the peak mode diameter is shifted towards smaller sizes. In presence of an OH scavenger the oxidation of 40.7 to 78.3 μg $m^{-3}$ limonene resulted in the production of 2.4 to 13.6 μg $m^{-3}$ SOA, respectively. As pointed out in Paper V the difference in the amount of limonene reacted (Δ limonene) between the two highest ozone levels (3500 and 5000 ppb) were only 0.9 μg $m^{-3}$ while the corresponding increase in SOA mass formed was 0.6 μg $m^{-3}$. This corresponds to a limonene SOA yield of approximately 0.66 which is unrealistically high at 298 K (Jonsson 2008; Saathoff et al. 2009) and implies that the additional conversion of the first generation limonene products occurs. It also results in a lower volatility of SOA.

The corresponding results for the same series of experiment without the use of an OH scavenger are in a similar way illustrated in Figure 17. The number size distributions shown as an insert in the figure illustrate a comparable effect of the increased ozone levels providing enhanced nucleation and a particle peak mode diameter shift towards smaller sizes. However, surprisingly the VFR was not at all influenced. The measured total SOA mass formed was larger than in the comparable experiments with OH scavenger and ranged from 12.1 to 27.1 μg $m^{-3}$ for low and high ozone experiments, respectively. The difference in the modelled Δ limonene was very small between the three highest ozone levels, indicating that the additional OH radical oxidation converts most of the limonene precursor even at lower ozone levels.

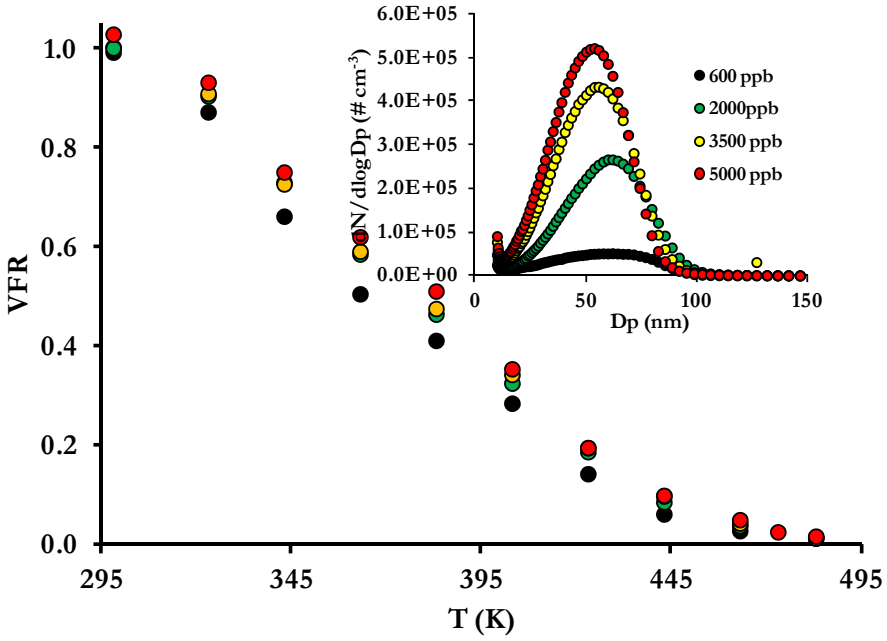


**Figure 16** The ozone concentration effect on SOA properties, with the use of 2-butanol as OH scavenger.

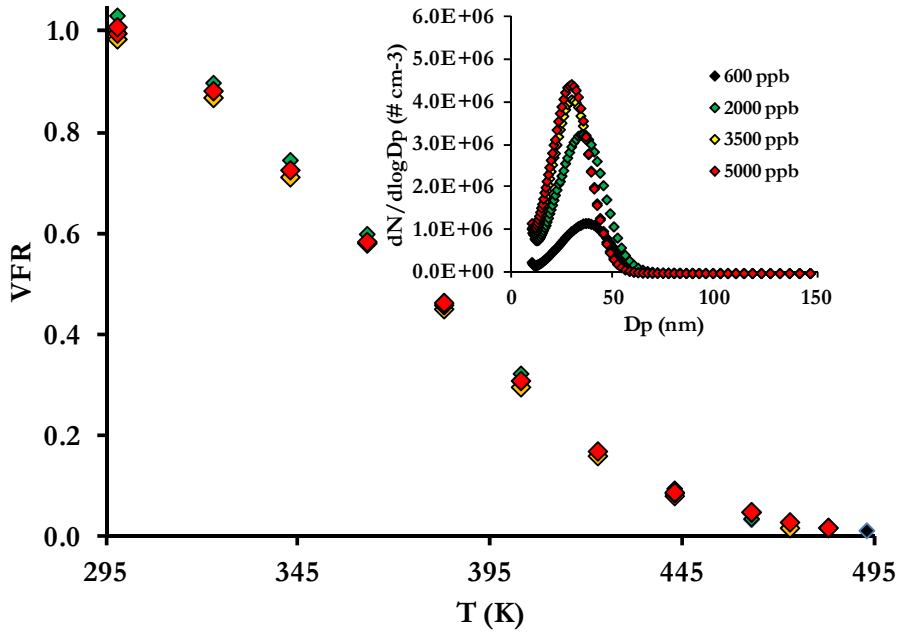


**Figure 17** The ozone concentration effect on SOA properties without the use of OH scavenger.

As seen in Paper V (Table 1) the kinetic model estimates the SOA masses in the experiments without scavenger to within 10% of the experimental values. However, it overestimates the SOA mass formed when an OH scavenger is used by 2-6 times. The measured SOA masses in the OH scavenger experiments were approximately 50% of the SOA masses measured in the corresponding experiments without OH scavenger. It seems that the model could not predict the measured negative effect on the SOA mass when a scavenger was used.

A positive effect of RH on the SOA formation yield from limonene ozonolysis have previously been demonstrated using the G-FROST laminar flow reactor (Jonsson et al. 2006; Jonsson et al. 2008b). In order to further evaluate this, a dry experiment (5% RH) was performed. The resulting VFR is illustrated in Paper V, (Figure 3) for limonene SOA at 5 and 40% RH, 5000 ppb ozone and using an OH scavenger. The VFR (383 K) for 55 nm particles increased with 5% in the dry condition experiment and this increase is larger than what can be attributed to just pure water uptake. This positive effect on the SOA volatility has also been reported by other studies as seen in Paper V and references therein. The additional water effect on the volatility is believed to be attributed to water induced changes in the reaction mechanisms.

## 4.3 Volatility of SOA from alkyl amines

Experiments were conducted to characterise SOA formed from the photooxidation reaction of a series of alkyl amines under low and high $NO_x$ conditions in the EUPHORE chamber facilities. The thermal properties of SOA formed from the gas phase photooxodation of mono-, di-, and trimethyl amine were evaluated within the ADA 2010 project. The main focus of this project was to understand the gas phase processes behind atmospheric amine degradation. In addition, goals of the project were to "assess the conditions for aerosol formation during the gas phase degradation of amines emitted to air, and to characterise and quantify the aerosol formation". Part of these experiments is described here within the scope of the thesis and linked to the work presented in Paper II. The focus is consequently on the results obtained using the VTDMA system, i.e. the thermal properties of the aerosol particles and to compare the volatility of the aerosol formed in the chamber experiments with the experiments of the pure aminium nitrate particles (Paper II).

#### 4.3.1 Precursor

The total aerosol mass yields in the photolysis experiments were similar for the three different precursors, around 8 – 9%, although significant differences in the thermal properties were observed. Monomethylamine formed the most volatile aerosol followed by dimethylamine and the least volatile aerosol was formed from the photooxidation of trimethylamine. The increasing order of VFR (383 K) measured after photooxodation was monomethylamine (49%) < dimethylamine (71%) < trimethylamine (82%). The volatility was also depending on the initial $NO_x$ conditions.

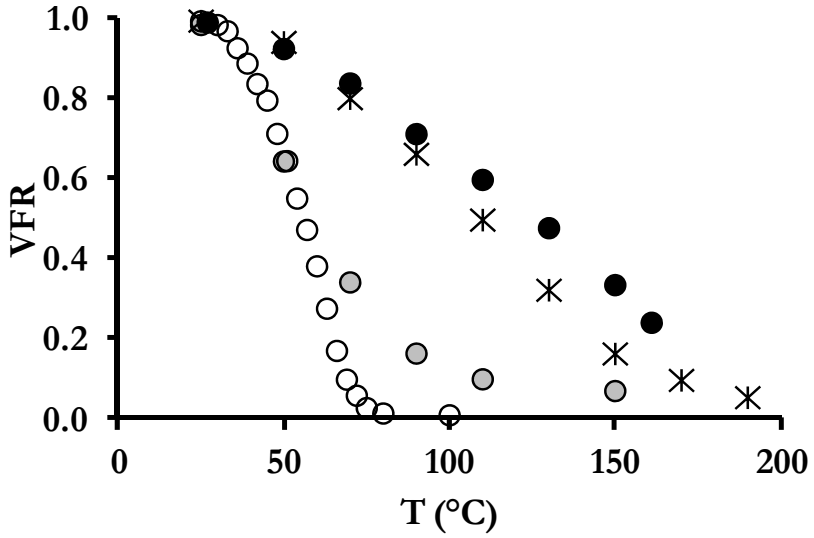


**Figure 18** Temperature dependence of the VFR of particles formed from the photooxidation of dimethylamine under high $NO_x$ (grey circles) and low $NO_x$ (black circles) conditions, in comparison with pure dimethylaminium nitrate particles (open circles) and α-pinene SOA (stars).

The thermograms in Figure 18 illustrate that the high $NO_x$ condition produce a more volatile salt-like aerosol while the low $NO_x$ condition aerosol is less volatile and resemble the SOA from monoterpene oxidation as described previously. This volatility effect was observed in the experiments with mono- and tri-methylamine but was most pronounced in the dimethylamine experiments.

### 4.3.2 Ageing

All of the performed experiments with alkylamines generated aerosol particles that were initially volatile. These volatile particles however became less volatile with time. This is illustrated in Figure 19 with the aerosol from a high $NO_x$ experiment using monomethylamine as a precursor. Thermograms were sampled 1, 3.3 and 4 hours after the start of the photooxidation. These thermograms are compared to a thermogram of a pure monomethylaminium nitrate aerosol from the experiments in Paper II.

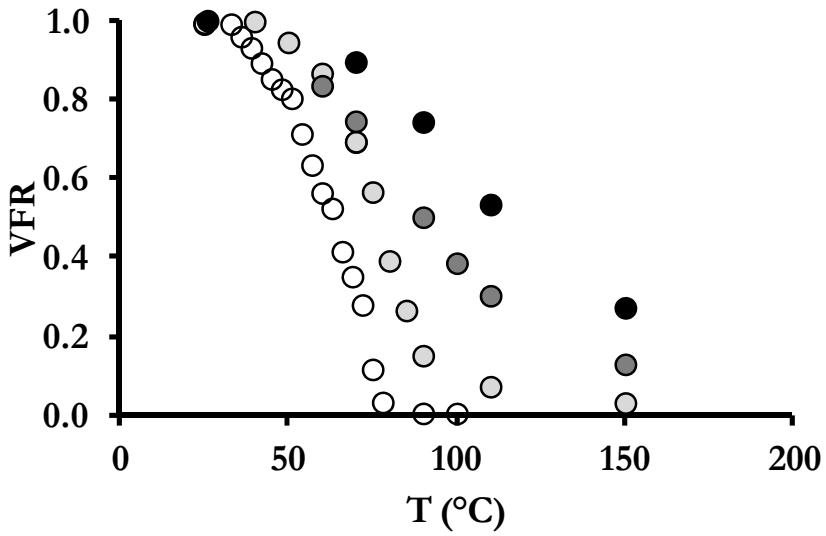


**Figure 19** Temperature dependence of the VFR of particles from photolysis of monomethylamine under high $NO_x$ conditions. VFR was measured, 1 (pale grey circles), 3.3 (dark grey circles) and 4 (black circles) hours after the start of the photooxidation. For comparison VFR for nebulised particles of pure monomethylaminium nitrate is shown (open circles).

The aerosol particles generated in the chamber experiments were characterised using an AMS. This characterisation of the photooxodation of monomethylamine showed that the contribution of the monomethylaminium nitrate signal to the total nitrate signal decreased from 65% to 35-40% during the experiment illustrated in Figure 19. This means that as much as 60-65% of the particle mass is not the initial amine salt but rather more classically secondary organic material at the end of the experiment. This increase in SOA contribution is in agreement with the observed decrease in volatility with time.

# 5. Conclusions

This work has demonstrated that the VTDMA system is a well suited instrument to measure physical properties, i.e. saturation vapour pressure and enthalpies of evaporisation, from nanosized aerosol samples of pure compounds in the vapour pressure range from $10^{-4}$ to $10^{-8}$ Pa. Another suited application is to characterise dynamic SOA properties and trace small changes due to aerosol processes. The results obtained with the VTDMA system in this work agree well with obtained results from other instruments used in parallel and with modelling work.

The SOA formed from ozonolysis of α-pinene and limonene is clearly semi-volatile and the gas phase part of the aerosol will get further oxidised by addition of OH radicals. It was demonstrated that the 2nd and 3rd generation of gas phase oxidation reactions to a large extent produce less volatile compounds compared to their parent compounds. These new oxidation products contribute to the SOA mass but form no new particles. However, the new SOA mass makes the particles more volatile in character, at least initially. When the gaseous compounds susceptible to OH-oxidation are consumed the mass increase stops and the VFR increases due to other ageing mechanisms, e.g. dilution and uptake onto chamber walls. The observed change in volatility agreed with the results obtained by chemical analysis of the condensed phase and by using the COSIMA model. The change in volatility was explained as a change in SOA composition, changing the relative contribution of compounds formed by the OH-oxidation to the pre-existing LVOC ozonolysis products.

These findings are in line with other chamber studies of e.g. engine exhaust aerosols by Robinson et al. (2007), where photooxodation of diluted primary organic aerosol (POA) doubled the condensed matter after three hours of photolytic initiated OH radical ageing. This implies that SVOC and IVOC from both primary and secondary sources can contribute to SOA formation. If the primary products from ozonolyis of limonene contains a double bond a second reaction with ozone may occur, reducing the volatility, but the effect of ozone on volatility diminish in the presence of OH radicals.

It is evident that the chemical composition of the SOA particle will have a large effect on its thermal properties. This implies that the physical properties of the single compounds that make up the SOA particle are important for the overall volatility of the aerosol particle. However, the phase of the evaporating particle will also influence the evaporation rate. This was seen in the experiments with pinonic acid described in Paper I where a small amount of impurities had a large effect on the evaporation rate. The experimental results presented within this work make it evident that gas-phase processes play an important role in the evolution of SOA. Many of the SOA components are semi-volatile and reactive, meaning that they can evaporate and get further oxidised. In order to understand these processes, the scientific understanding must embrace everything from properties of pure compounds, via simplified experimental conditions all the way to the complex processes in the atmosphere.

It is evident that more characterisation of pure SOA components is needed in order to improve models and databases used to estimate physical properties of unknown compounds. Hopefully the physical properties obtained can be useful in the work of understanding the global aerosol budget and the contribution from secondary reactions.

## Acknowledgements

First of all I would like to thank my head supervisor Professor Mattias Hallquist that, apart from being a talented scientist and an encouraging and patient supervisor, is a really nice guy. Secondly I would like to thank my two assistant supervisors Dr Åsa Jonsson and Dr Patrik Andersson. Åsa is always very competent and helpful disregarding of her own working load. And I don't think that I have yet presented Patrik a problem that he could not help me to solve, if not at once so within an hour or two. Thank you all for support and input during the work with this thesis.

I also want to acknowledge the next door neighbour, my examiner Professor Evert Ljungström, filled up to the brim with knowledge, wisdom and with admirable skills in the laboratory.

And a big thanks to all friends and colleagues that is or has been a part of the Atmospheric Science group, you have been making it a friendly and fruitful workplace. Keep up the good work! There are still a lot of things in the air, waiting to be discovered and characterised.

All colleagues at the AIDA, SAPHIR and EUPHORE chambers, thank you for giving me the great opportunity to take part in your work and learn how things are done in the big wide world.

I am also very grateful for all support and love from friends, neighbours and family.

This work was made possible by financial support from: Formas under contract 214-2006-1204, The Swedish Research Council under contract 80475101, and The Nanoparticles in Interactive Environments platform at the Faculty of Science at the University of Gothenburg. The research presented is a contribution to the Swedish strategic research area ModElling the Regional and Global Earth system, MERGE.

Ångpanneföreningen, EUROCHAMP, Filosofiska fakulteternas gemensamma donationsnämnd (Göteborgs Universitet) and Knut and Alice Wallenbergs Foundation are acknowledged for generous travel grants.

## Bibliography


Aiken, A. C., P. F. DeCarlo, J. H. Kroll, D. R. Worsnop, J. A. Huffman, K. S. Docherty, I. M. Ulbrich, C. Mohr, J. R. Kimmel, D. Sueper, Y. Sun, Q. Zhang, A. Trimborn, M. Northway, P. J. Ziemann, M. R. Canagaratna, T. B. Onasch, M. R. Alfarra, A. S. H. Prevot, J. Dommen, J. Duplissy, A. Metzger, U. Baltensperger and J. L. Jimenez (2008).O/C and OM/OC Ratios of Primary, Secondary, and Ambient Organic Aerosols with High-Resolution Time-of-Flight Aerosol Mass Spectrometry. Environmental Science and Technology **42**(12): 4478.

Arneth, A., S. P. Harrison, S. Zaehle, K. Tsigaridis, S. Menon, P. J. Bartlein, J. Feichter, A. Korhola, M. Kulmala, D. O'Donnell, G. Schurgers, S. Sorvari and T. Vesala (2010).Terrestrial biogeochemical feedbacks in the climate system. Nature Geosci **3**(8): 525.

Atkinson, R., J. Arey and S. M. Aschmann (2008).Atmospheric chemistry of alkanes: Review and recent developments. Atmospheric Environment **42**(23): 5859.

Barley, M. H. and G. McFiggans (2010).The critical assessment of vapour pressure estimation methods for use in modelling the formation of atmospheric organic aerosol. Atmospheric Chemistry and Physics **10**(2): 749.

Barsanti, K. C. and J. F. Pankow (2004).Thermodynamics of the formation of atmospheric organic particulate matter by accretion reactions--Part 1: aldehydes and ketones. Atmospheric Environment **38**(26): 4371.

Barsanti, K. C. and J. F. Pankow (2005).Thermodynamics of the formation of atmospheric organic particulate matter by accretion reactions--2. Dialdehydes, methylglyoxal, and diketones. Atmospheric Environment **39**(35): 6597.

Barsanti, K. C. and J. F. Pankow (2006).Thermodynamics of the formation of atmospheric organic particulate matter by accretion reactions--Part 3: Carboxylic and dicarboxylic acids. Atmospheric Environment **40**(34): 6676.

Bateman, A. P., S. A. Nizkorodov, J. Laskin and A. Laskin (2011).Photolytic processing of secondary organic aerosols dissolved in cloud droplets. Physical Chemistry Chemical Physics **13**(26): 12199.

Bilde, M. and S. N. Pandis (2001).Evaporation Rates and Vapor Pressures of Individual Aerosol Species Formed in the Atmospheric Oxidation of a- and b-Pinene. Environmental Science and Technology **35**(16): 3344.

Bilde, M., B. Svenningsson, J. Monster and T. Rosenorn (2003).Even-Odd Alternation of Evaporation Rates and Vapor Pressures of C3-C9 Dicarboxylic Acid Aerosols. Environmental Science & Technology **37**(7): 1371.

Bird, R. B., W. E. Stewart and E. N. Lightfoot (1960). In Transport Phenomena. New York, Wiley.

Burger, A., J. O. Henck and M. N. Dunser (1996).On the polymorphism of dicarboxylic acids: I pimelic acid. Mikrochimica Acta **122**(3-4): 247.

Calvert, J. G. (2000). The mechanisms of atmospheric oxidation of the alkenes, Oxford University Press.

Chattopadhyay, S. and P. J. Ziemann (2005).Vapor pressures of substituted and unsubstituted monocarboxylic and dicarboxylic acids measured using an improved thermal desorption particle beam mass spectrometry method. Aerosol Science and Technology **39**(11): 1085.

Chen, Q., Y. Liu, N. M. Donahue, J. E. Shilling and S. T. Martin (2011).Particle-Phase Chemistry of Secondary Organic Material: Modeled Compared to Measured O:C and H:C Elemental Ratios Provide Constraints. Environmental Science & Technology **45**(11): 4763.

Chien, W.-M., D. Chandra, K. H. Lau, D. L. Hildenbrand and A. M. Helmy (2010).The vaporization of NH4NO3. Journal of Chemical Thermodynamics **42**(7): 846.

Claeys, M., R. Szmigielski, I. Kourtchev, P. Van der Veken, R. Vermeylen, W. Maenhaut, M. Jaoui, T. E. Kleindienst, M. Lewandowski, J. H. Offenberg and E. O. Edney (2007).Hydroxydicarboxylic Acids:As Markers for Secondary Organic Aerosol from the Photooxidation of α-Pinene. Environmental Science & Technology **41**(5): 1628.

DeCarlo, P. F., J. R. Kimmel, A. Trimborn, M. J. Northway, J. T. Jayne, A. C. Aiken, M. Gonin, K. Fuhrer, T. Horvath, K. S. Docherty, D. R. Worsnop and J. L. Jimenez (2006).Field-Deployable, High-Resolution, Time-of-Flight Aerosol Mass Spectrometer. Analytical Chemistry **78**(24): 8281.

Donahue, N. M., A. L. Robinson, C. O. Stanier and S. N. Pandis (2006). Coupled Partitioning, Dilution, and Chemical Aging of Semivolatile Organics. Environmental Science & Technology **40:** 2635.

Fenger, J. (2009).Air pollution in the last 50 years – From local to global. Atmospheric Environment **43**(1): 13.

Finlayson-Pitts, B. J. and J. N. Pitts Jr (2000). Chapter 1 - Overview of the Chemistry of Polluted and Remote Atmospheres. Chemistry of the Upper and Lower Atmosphere. San Diego, Academic Press**:** 1.

Fuchs, N. A. (1963).On the stationary charge distribution on aerosol particles in a bipolar ionic atmosphere. Pure and Applied Geophysics **56**(1): 185.

Fuchs, N. A. and A. G. Sutugin (1971). Topics in Current Aerosol Research. G. N. Hidy and J. R. Brock. New York, Pergamon Press.

Ge, X., A. S. Wexler and S. L. Clegg (2011).Atmospheric amines - Part I. A review. Atmospheric Environment **45**(3): 524.

George, I. J. and J. P. D. Abbatt (2010).Heterogeneous oxidation of atmospheric aerosol particles by gas-phase radicals. Nat Chem **2**(9): 713.

Geron, C., R. Rasmussen, R. R. Arnts and A. Guenther (2000).A review and synthesis of monoterpene speciation from forests in the United States. Atmospheric Environment **34**(11): 1761.

Goldstein, A. H. and I. E. Galbally (2007).Known and unexplored organic constituents in the Earth's atmosphere. Environmental Science & Technology **41**(5): 1514.

Gravatt, C. C., P. D. La Fleur and K. F. J. Heinrich (1977). Proceedings of Workshop on Asbestos: Definitions and Measurment Methods, Gaithersburg, Maryland U.S., U.S. Departement of Commerce.

Guenther, A., C. N. Hewitt, D. Erickson, R. Fall, C. Geron, T. Graedel, P. Harley, L. Klinger, M. Lerdau, W. A. McKay, T. Pierce, B. Scholes, R. Steinbrecher, R. Tallamraju, J. Taylor and P. Zimmerman (1995).A global model of natural volatile organic compound emissions. J. Geophys. Res. **100**(D5): 8873.

Hallquist, M., J. C. Wenger, U. Baltensperger, Y. Rudich, D. Simpson, M. Claeys, J. Dommen, N. M. Donahue, C. George, A. H. Goldstein, J. F. Hamilton, H. Herrmann, T. Hoffmann, Y. Iinuma, M. Jang, M. E. Jenkin, J. L. Jimenez, A. Kiendler-Scharr, W. Maenhaut, G. McFiggans, T. F. Mentel, A. Monod, A. S. H. Prévôt, J. H. Seinfeld, J. D. Surratt, R. Szmigielski and J. Wildt (2009).The formation, properties and impact of secondary organic aerosol: current and emerging issues. Atmospheric Chemistry and Physics **9**(14): 5155.

Hinds, W. C. (1999). Aerosol technology: properties, behavior, and measurement of airborne particles, Wiley.

Imrich, A., N. Yao Yu and L. Kobzik (2000).Insoluble components of concentrated air particles mediate alveolar macrophage responses in vitro. Toxicology and Applied Pharmacology **167**(2): 140.

Jayne, J. T., D. C. Leard, X. F. Zhang, P. Davidovits, K. A. Smith, C. E. Kolb and D. R. Worsnop (2000).Development of an aerosol mass spectrometer for size and composition analysis of submicron particles. Aerosol Science and Technology **33**(1-2): 49.

Jiang, L., W. Wang and Y. Xu (2010).Ab initio investigation of O3 addition to double bonds of limonene. Chemical Physics **368**(3): 108.

Jimenez, J. L., M. R. Canagaratna, N. M. Donahue, A. S. H. Prevot, Q. Zhang, J. H. Kroll, P. F. DeCarlo, J. D. Allan, H. Coe, N. L. Ng, A. C. Aiken, K. S. Docherty, I. M. Ulbrich, A. P. Grieshop, A. L. Robinson, J. Duplissy, J. D. Smith, K. R. Wilson, V. A. Lanz, C. Hueglin, Y. L. Sun, J. Tian, A. Laaksonen, T. Raatikainen, J. Rautiainen, P. Vaattovaara, M. Ehn, M. Kulmala, J. M. Tomlinson, D. R. Collins, M. J. Cubison, E, J. Dunlea, J. A. Huffman, T. B. Onasch, M. R. Alfarra, P. I. Williams, K. Bower, Y. Kondo, J. Schneider, F. Drewnick, S. Borrmann, S. Weimer, K. Demerjian, D. Salcedo, L. Cottrell, R. Griffin, A. Takami, T. Miyoshi, S. Hatakeyama, A. Shimono, J. Y. Sun, Y. M. Zhang, K. Dzepina, J. R. Kimmel, D. Sueper, J. T. Jayne, S. C. Herndon, A. M. Trimborn, L. R. Williams, E. C. Wood, A. M. Middlebrook, C. E. Kolb, U. Baltensperger and D. R. Worsnop (2009).Evolution of Organic Aerosols in the Atmosphere. Science **326**(5959): 1525.

Johnson, D. and G. Marston (2008).The gas-phase ozonolysis of unsaturated volatile organic compounds in the troposphere. Chemical Society Reviews **37**(4): 699.

Jonsson, Å. M. (2008). Physical and Chemical Processes in the Formation of Biogenic Secondary Organic Aerosols, University of Gothenburg.

Jonsson, Å. M., M. Hallquist and E. Ljungström (2006).Impact of Humidity on the Ozone Initiated Oxidation of Limonene, D3-Carene, and a-Pinene. Environmental Science and Technology **40**(1): 188.

Jonsson, Å. M., M. Hallquist and E. Ljungström (2008a).Influence of OH Scavenger on the Water Effect on Secondary Organic Aerosol Formation from Ozonolysis of Limonene, Δ3-Carene, and α-Pinene. Environmental Science & Technology **42**(16): 5938.

Jonsson, Å. M., M. Hallquist and E. Ljungström (2008b).The effect of temperature and water on secondary organic aerosol formation from ozonolysis of limonene, Δ3-carene and α-pinene. Atmos. Chem. Phys. **8**(21): 6541.

Jonsson, Å. M., M. Hallquist and H. Saathoff (2007).Volatility of secondary organic aerosols from the ozone initiated oxidation of [alpha]-pinene and limonene. Journal of Aerosol Science **38**(8): 843.

Jordan, C., E. Fitz, T. Hagan, B. Sive, E. Frinak, K. Haase, L. Cottrell, S. Buckley and R. Talbot (2009).Long-term study of VOCs measured with PTR-MS at a rural site in New Hampshire with urban influences. Atmos. Chem. Phys. **9**(14): 4677.

Kalberer, M., D. Paulsen, M. Sax, M. Steinbacher, J. Dommen, A. S. H. Prevot, R. Fisseha, E. Weingartner, V. Frankevich, R. Zenobi and U. Baltensperger (2004).Identification of Polymers as Major Components of Atmospheric Organic Aerosols. Science **303**(5664): 1659.

Kanakidou, M., J. H. Seinfeld, S. N. Pandis, I. Barnes, F. J. Dentener, M. C. Facchini, R. Van Dingenen, B. Ervens, A. Nenes, C. J. Nielsen, E. Swietlicki, J. P. Putaud, Y. Balkanski, S. Fuzzi, J. Horth, G. K. Moortgat, R. Winterhalter, C. E. L. Myhre, K. Tsigaridis, E. Vignati, E. G. Stephanou and J. Wilson (2005).Organic aerosol and global climate modelling: a review. Atmospheric Chemistry and Physics **5**(4): 1053.

Koponen, I. K., I. Riipinen, A. Hienola, M. Kulmala and M. Bilde (2007).Thermodynamic Properties of Malonic, Succinic, and Glutaric Acids: Evaporation Rates and Saturation Vapor Pressures. Environmental Science & Technology **41**(11): 3926.

Kulmala, M., H. Vehkamäki, T. Petäjä, M. Dal Maso, A. Lauri, V. M. Kerminen, W. Birmili and P. H. McMurry (2004).Formation and growth rates of ultrafine atmospheric particles: a review of observations. Journal of Aerosol Science **35**(2): 143.

Kurtén, T., V. Loukonen, H. Vehkamäki and M. Kulmala (2008).Amines are likely to enhance neutral and ion-induced sulfuric acid-water nucleation in the atmosphere more effectively than ammonia. Atmospheric Chemistry and Physics **8**(14): 4095.

Lambe, A. T., M. A. Miracolo, C. J. Hennigan, A. L. Robinson and N. M. Donahue (2009).Effective Rate Constants and Uptake Coefficients for the Reactions of Organic Molecular Markers (n-Alkanes, Hopanes, and Steranes) in Motor Oil and Diesel Primary Organic Aerosols with Hydroxyl Radicals. Environmental Science & Technology **43**(23): 8794.

Lambe, A. T., J. Zhang, A. M. Sage and N. M. Donahue (2007).Controlled OH Radical Production via Ozone-Alkene Reactions for Use in Aerosol Aging Studies. Environmental Science & Technology **41**(7): 2357.

Li, Q., D. Hu, S. Leungsakul and R. M. Kamens (2007).Large outdoor chamber experiments and computer simulations: (I) Secondary organic aerosol formation from the oxidation of a mixture of d-limonene and α-pinene. Atmospheric Environment **41**(40): 9341.
Lindinger, W., A. Hansel and A. Jordan (1998).On-line monitoring of volatile organic compounds at pptv levels by means of proton-transfer-reaction mass spectrometry (PTR-MS) medical applications, food control and environmental research. International Journal of Mass Spectrometry and Ion Processes **173**(3): 191.
Lloyd, J. A., K. J. Heaton and M. V. Johnston (2009).Reactive Uptake of Trimethylamine into Ammonium Nitrate Particles. Journal of Physical Chemistry A **113**(17): 4840.
Löndahl, J., A. Massling, E. Swietlicki, E. V. Bräuner, M. Ketzel, J. Pagels and S. Loft (2009).Experimentally Determined Human Respiratory Tract Deposition of Airborne Particles at a Busy Street. Environmental Science & Technology **43**(13): 4659.
Lutgens, F. K. and E. J. Tarbuck (2004). The Atmosphere: An Introduction to Meteorology. Upper Saddle River, New Jersey, Prentice Hall.
Ma, Y., T. R. Willcox, A. T. Russell and G. Marston (2007).Pinic and pinonic acid formation in the reaction of ozone with a-pinene. Chemical Communications (Cambridge, United Kingdom)(13): 1328.
Matsunaga, A. and P. J. Ziemann (2010).Gas-Wall Partitioning of Organic Compounds in a Teflon Film Chamber and Potential Effects on Reaction Product and Aerosol Yield Measurements. Aerosol Science and Technology **44**(10): 881
Mikhailov, E., S. Vlasenko, S. T. Martin, T. Koop and U. Pöschl (2009).Amorphous and crystalline aerosol particles interacting with water vapor: conceptual framework and experimental evidence for restructuring, phase transitions and kinetic limitations. Atmospheric Chemistry and Physics **9**(24): 9491.
Müller, L., M. C. Reinnig, K. H. Naumann, H. Saathoff, T. F. Mentel, N. M. Donahue and T. Hoffmann (2011).Formation of 3-methyl-1,2,3-butanetricarboxylic acid via gas phase oxidation of pinonic acid – a mass spectrometric study of SOA aging. Atmos. Chem. Phys. Discuss. **11**(7): 19443.
Naumann, K.-H. (2003).COSIMA--a computer program simulating the dynamics of fractal aerosols. Journal of Aerosol Science **34**(10): 1371.
Nielsen, C. J., B. D'Anna, M. Aursnes, A. Boreave, R. Bossi, A. J. C. Bunkan, M. Glasius, M. Hallquist, M. Karl, K. Kristensen, T. Mikoviny, M. M. Maguta, M. Müller, J. Westerlund, K. Salo, Y. Stenstrøm and A. Wisthaler (2010). Atmospheric Degradation of Amines (ADA), CLIMIT project no. 201604.
Pankow, J. F. (1994).An absorption model of gas/particle partitioning of organic compounds in the atmosphere. Atmospheric Environment **28**(2): 185.
Peñuelas, J. and M. Staudt (2010).BVOCs and global change. Trends in plant science **15**(3): 133.
Pope, C. A. and D. W. Dockery (2006).Health effects of fine particulate air pollution: Lines that connect. Journal of the Air & Waste Management Association **56**(6): 709.
Pöschl, U. (2005).Atmospheric aerosols: Composition, transformation, climate and health effects. Angewandte Chemie-International Edition **44**(46): 7520.
Pöschl, U. (2011).Gas-particle interactions of tropospheric aerosols: Kinetic and thermodynamic perspectives of multiphase chemical reactions, amorphous organic substances, and the activation of cloud condensation nuclei. Atmospheric Research **101**(3): 562.
Pöschl, U., Y. Rudich and M. Ammann (2007).Kinetic model framework for aerosol and cloud surface chemistry and gas-particle interactions.; Part 1: General equations, parameters, and terminology. Atmos. Chem. Phys. **7**(23): 5989.
Rasch, P. J., P. J. Crutzen and D. B. Coleman (2008).Exploring the geoengineering of climate using stratospheric sulfate aerosols: The role of particle size. Geophysical Research Letters **35**(2): L02809.
Riipinen, I., J. R. Pierce, N. M. Donahue and S. N. Pandis (2010).Equilibration time scales of organic aerosol inside thermodenuders: Evaporation kinetics versus thermodynamics. Atmospheric Environment **44**(5): 597.
Robinson, A. L., N. M. Donahue, M. K. Shrivastava, E. A. Weitkamp, A. M. Sage, A. P. Grieshop, T. E. Lane, J. R. Pierce and S. N. Pandis (2007).Rethinking Organic Aerosols: Semivolatile Emissions and Photochemical Aging. Science **315**(5816): 1259.

Rohrer, F., B. Bohn, T. Brauers, D. Brüning, F. J. Johnen, A. Wahner and J. Kleffmann (2005).Characterisation of the photolytic HONO-source in the atmosphere simulation chamber SAPHIR. Atmospheric. Chemistry and Physiscs **5**(6): 2189.

Rollins, A. W., A. Kiendler-Scharr, J. L. Fry, T. Brauers, S. S. Brown, H. P. Dorn, W. P. Dubé, H. Fuchs, A. Mensah, T. F. Mentel, F. Rohrer, R. Tillmann, R. Wegener, P. J. Wooldridge and R. C. Cohen (2009).Isoprene oxidation by nitrate radical: alkyl nitrate and secondary organic aerosol yields. Atmospheric Chemistry and Physics **9**(18): 6685.

Russell, A. G. and B. Brunekreef (2009).A Focus on Particulate Matter and Health. Environmental Science & Technology **43**(13): 4620.

Saathoff, H., K. H. Naumann, O. Möhler, Å. M. Jonsson, M. Hallquist, A. Kiendler-Scharr, T. F. Mentel, R. Tillmann and U. Schurath (2009).Temperature dependence of yields of secondary organic aerosols from the ozonolysis of α-pinene and limonene. Atmospheric Chemistry and Physics **9**(5): 1551.

Saleh, R., A. Khlystov and A. Shihadeh (2011).Determination of Evaporation Coefficients of Ambient and Laboratory-Generated Semivolatile Organic Aerosols from Phase Equilibration Kinetics in a Thermodenuder. Aerosol Science and Technology **46**(1): 22.

Saleh, R., A. Shihadeh and A. Khlystov (2009).Determination of evaporation coefficients of semi-volatile organic aerosols using an integrated volume--tandem differential mobility analysis (IV-TDMA) method. Journal of Aerosol Science **40**(12): 1019.

Saleh, R., J. Walker and A. Khlystov (2008).Determination of saturation pressure and enthalpy of vaporization of semi-volatile aerosols: The integrated volume method. Journal of Aerosol Science **39**(10): 876.

Schurgers, G., A. Arneth, R. Holzinger and A. H. Goldstein (2009).Process-based modelling of biogenic monoterpene emissions combining production and release from storage. Atmospheric Chemistry and Physics **9**(10): 3409.

Seinfeld, J. H. and S. N. Pandis (2006). Atmospheric chemistry and physics: from air pollution to climate change, Wiley.

Shiraiwa, M., M. Ammann, T. Koop and U. Pöschl (2011).Gas uptake and chemical aging of semisolid organic aerosol particles. Proceedings of the National Academy of Sciences **108**(27): 11003.

Sjögren, S., M. Gysel, E. Weingartner, U. Baltensperger, M. J. Cubison, H. Coe, A. A. Zardini, C. Marcolli, U. K. Krieger and T. Peter (2007).Hygroscopic growth and water uptake kinetics of two-phase aerosol particles consisting of ammonium sulfate, adipic and humic acid mixtures. Journal of Aerosol Science **38**(2): 157.

Smith, J. N., K. C. Barsanti, H. R. Friedli, M. Ehn, M. Kulmala, D. R. Collins, J. H. Scheckman, B. J. Williams and P. H. McMurry (2010).Observations of aminium salts in atmospheric nanoparticles and possible climatic implications. Proceedings of the National Academy of Sciences of the United States of America **107**(15): 6634.

Solomon, S., D. Qin, M. Manning, M. M. Z. Chen, K. B. Averyt, M.Tignor and H. L. Miller (2007). IPCC, 2007: Climate Change 2007: The Physical Science Basis. Contribution of Working Group I to the Fourth Assessment Report of the Intergovernmental Panel on Climate Change. C. U. Press. Cambridge.

Thalladi, V. R., M. Nusse and R. Boese (2000). The melting point alternation in alpha,omega-alkanedicarboxylic acids. Journal of the American Chemical Society **122:** 9227.

Thitakamol, B., A. Veawab and A. Aroonwilas (2007).Environmental impacts of absorption-based CO2 capture unit for post-combustion treatment of flue gas from coal-fired power plant. International Journal of Greenhouse Gas Control **1**(3): 318.

Tolocka, M. P., M. Jang, J. M. Ginter, F. J. Cox, R. M. Kamens and M. V. Johnston (2004).Formation of Oligomers in Secondary Organic Aerosol. Environmental Science & Technology **38**(5): 1428.

Vaden, T. D., D. Imre, J. Beránek, M. Shrivastava and A. Zelenyuk (2011).Evaporation kinetics and phase of laboratory and ambient secondary organic aerosol. Proceedings of the National Academy of Sciences **108**(6): 2190.

Virtanen, A., J. Joutsensaari, T. Koop, J. Kannosto, P. Yli-Pirila, J. Leskinen, J. M. Makela, J. K. Holopainen, U. Poschl, M. Kulmala, D. R. Worsnop and A. Laaksonen (2010).An amorphous solid state of biogenic secondary organic aerosol particles. Nature **467**(7317): 824.

Zhang, Y. Y., L. Müller, R. Winterhalter, G. K. Moortgat, T. Hoffmann and U. Pöschl (2010).Seasonal cycle and temperature dependence of pinene oxidation products, dicarboxylic acids and nitrophenols in fine and coarse air particulate matter. Atmos. Chem. Phys. **10**(16): 7859.
Zobrist, B., C. Marcolli, D. A. Pedernera and T. Koop (2008).Do atmospheric aerosols form glasses? Atmospheric Chemistry and Physics **8**(17): 5221.